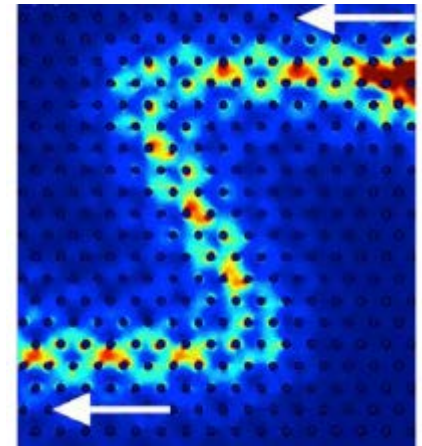
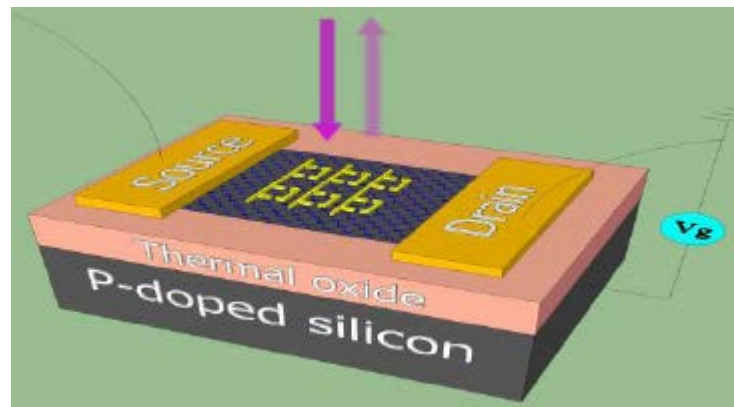
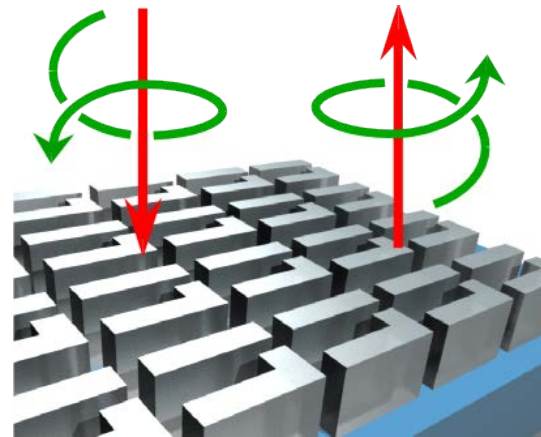




Metamaterials-Inspired Electromagnetics and Photonics

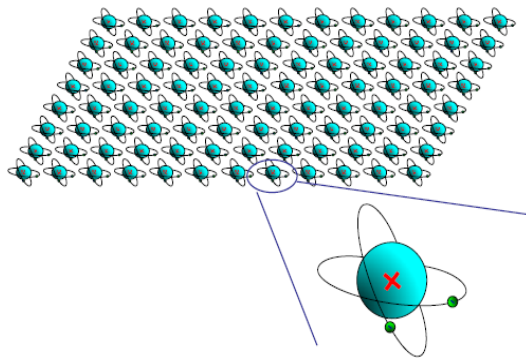
Gennady Shvets, The University of Texas at Austin



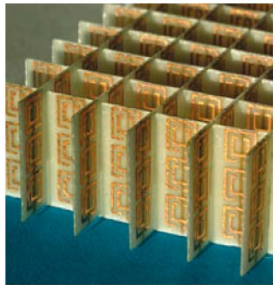
**Condensed Matter and Materials Research Committee Spring Meeting,
National Academies' Keck Center, Washington, DC, May 1, 2014**



Meta-Materials: Mesoscopic EM Materials



Natural materials: unit cell is an atom \ll radiation wavelength

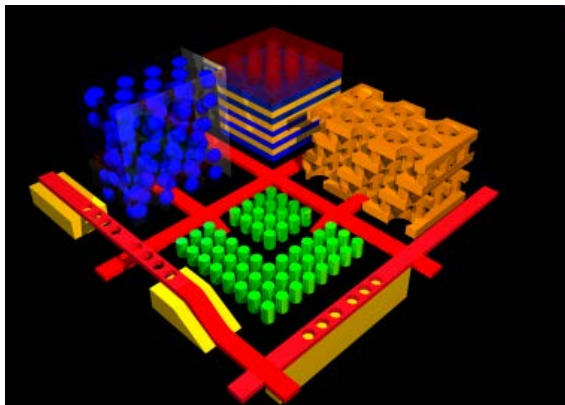


MetaMaterials: atom \ll unit cell $< \lambda$

Unit cell is small enough \rightarrow effective medium description (homogenization, constitutive parameters ϵ, μ)

Carefully designed resonant unit cells (e.g. split rings etc.)

Remarkable optical/EM properties enabled by finite cell size \rightarrow spatial dispersion, optical magnetism, bi-anisotropy

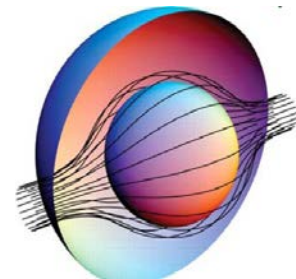
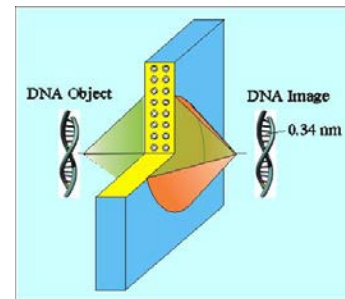
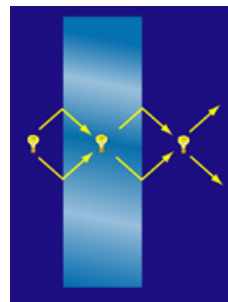


Photonic crystals: unit cell is sized to $\frac{1}{2}$ of the radiation wavelength

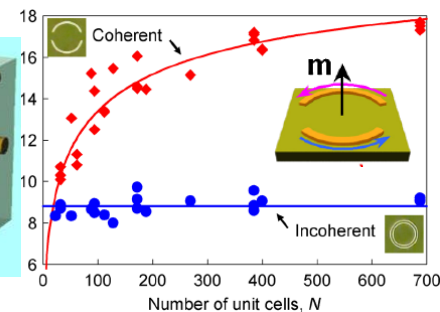
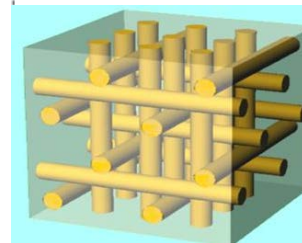
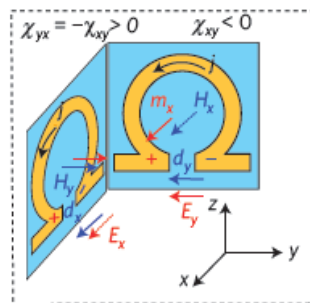


Evolution of Metamaterials Research

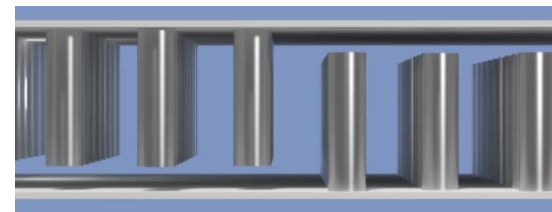
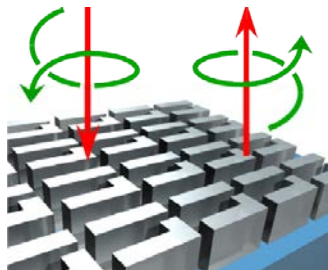
•Early days: focus on exotic bulk properties → negative refractive index, super-lensing, “cloaking”



•Understanding of the EM properties of MMs and their building blocks: high-frequency magnetism, bi-anisotropy, homogenization



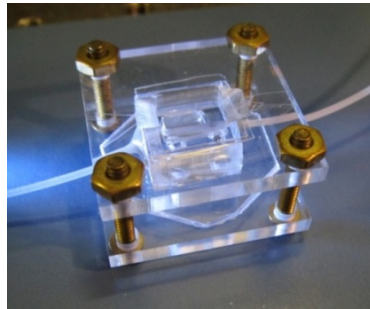
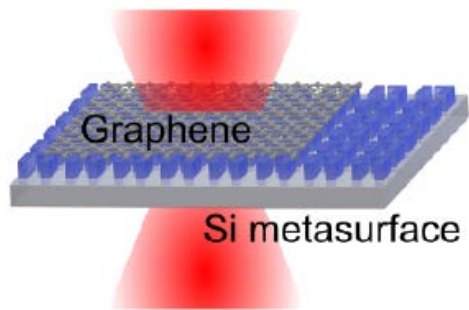
•Modern Era: Metamaterials-inspired Electromagnetics in two and three dimensions





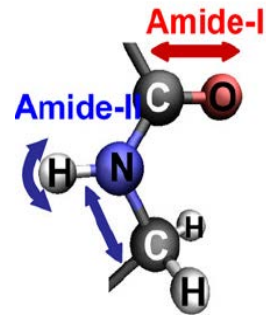
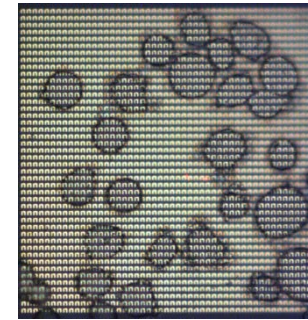
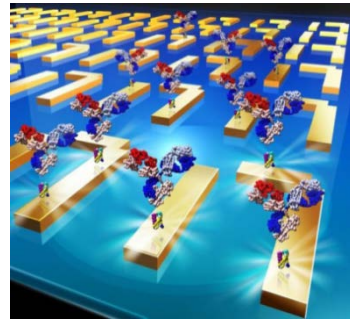
Spectrally Selective Field-Concentrating Optical Resonators Inspired by MMs

High-Precision graphene spectroscopy and ultrafast optoelectronic devices



Wu et. al. (Shvets), Nature Comm. (2014, in print)

IR Bio-Spectroscopy: from designing better immunosensors to single-cell fingerprinting



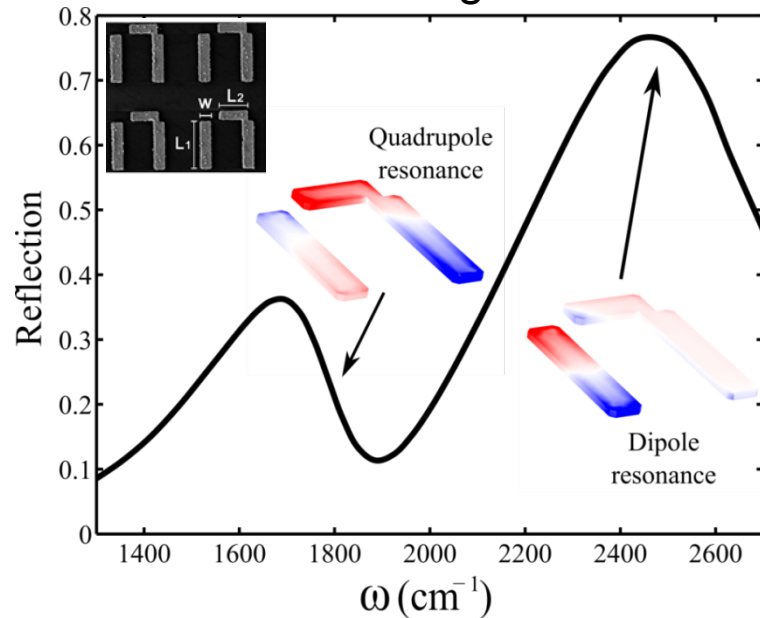
Wu et. al. (Altug & Shvets), Nature Mat. **11**, 69 (2012)

- Narrow resonances (high-Q) + Strong field enhancements → Small changes of local environment can strongly affect optical response
- Controlling optical response using minute amounts of material, e.g. atomic monolayer of graphene, protein monolayers
- Ultra-sensitive fingerprinting/characterization of trace amounts of biological matter (protein monolayers, single cells, etc.)

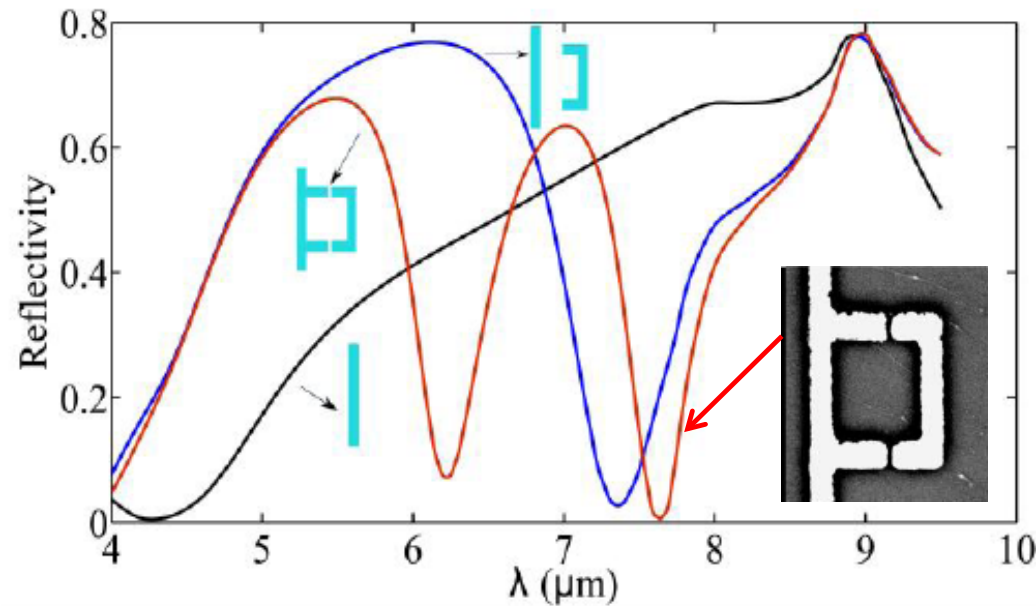


Meta-Surfaces Based on Split Rings

One dark and one bright resonance

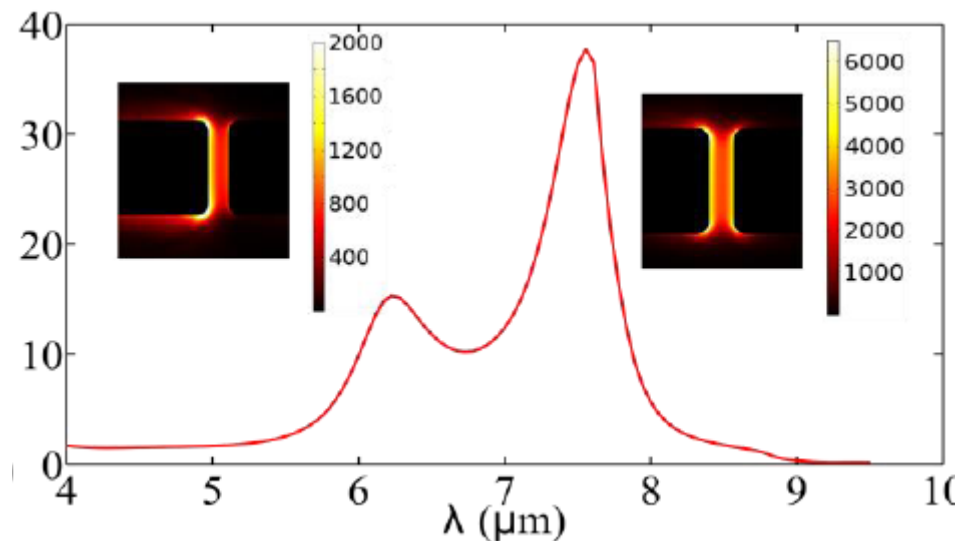


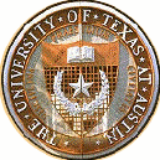
Continuum + 2 dark resonances



Easy to turn “Fano”-resonant metasurfaces into active ones:

- (a) Strong field enhancement → small amounts of active material (e.g., graphene) is needed**
- (b) Even small spectral shifts translate into large changes in transmission/reflection**





Outline of the Talk

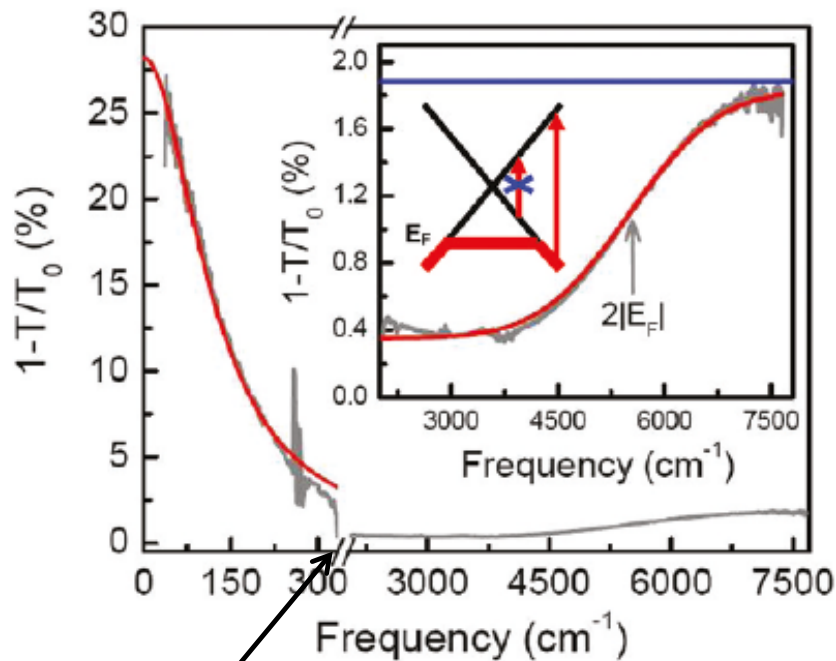
- **Plasmonic Meta-Surfaces Functionalized with Graphene**
- **The All-Dielectric Metasurfaces: Beating the Ohmic Loss**
- **Emulating the electron spin in photons using metamaterials: Photonic Topological Insulators**
- **Metamaterials-enhanced IR spectroscopy in life sciences: from proteins to cells**

Metamaterials and metamaterials-inspired photonic structures are already contributing to investigating condensed and soft matter materials such as graphene, proteins, cells

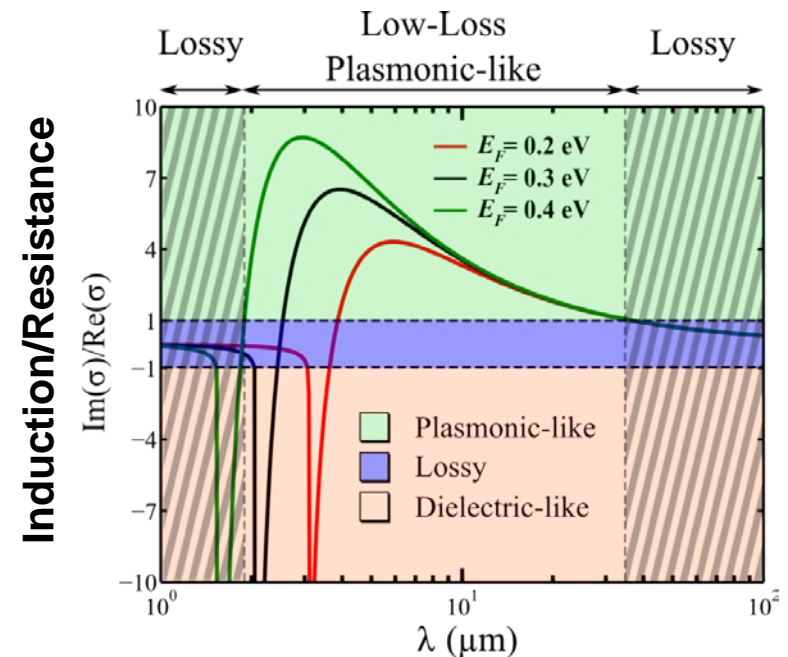
They may soon contribute to emulating many-body interactions in condensed matter systems such as topological insulators

The most exciting future work is likely to be done at the meso-scale, e.g., “slightly” sub-wavelength, “somewhat” coherent MMs interacting with wavelength-scale objects (i.e. biological cells)

Mid-IR Meta-Surfaces Enhance Graphene's Response and Can be Controlled by SLG



SLG's mid-IR response is weak: small Drude conductivity and no interband transitions, but...

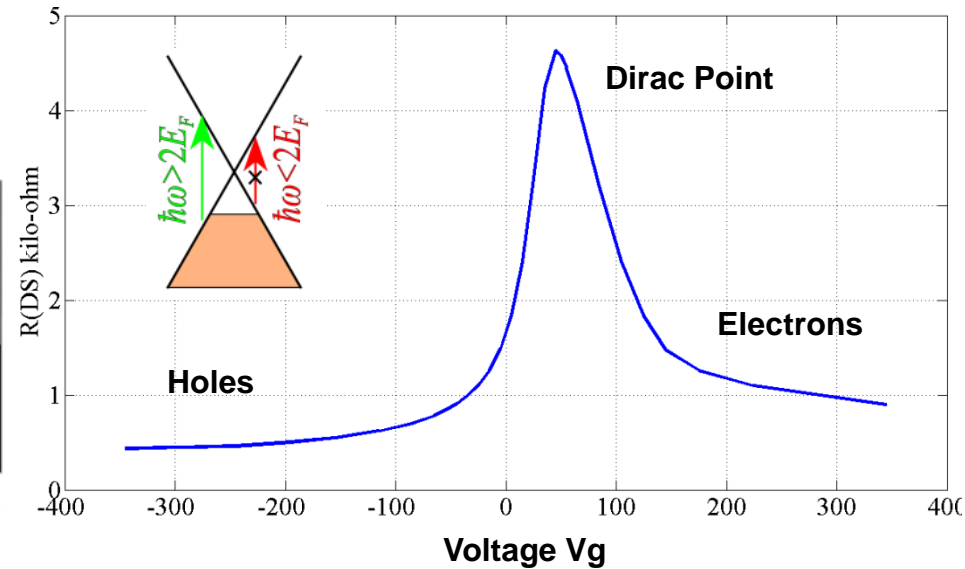
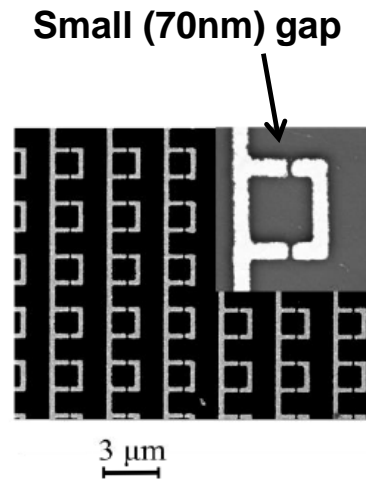
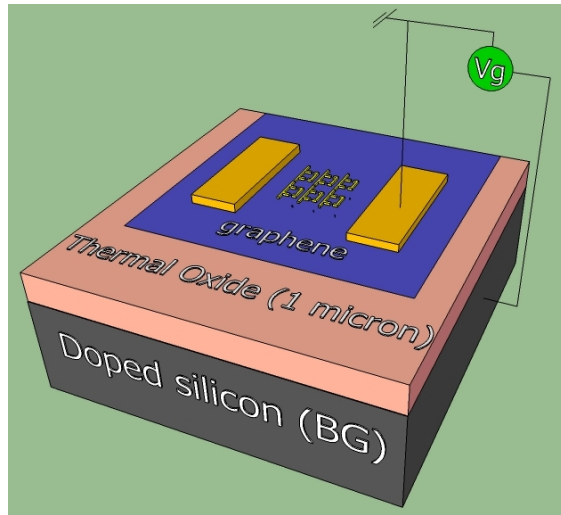


Graphene is a low-loss plasmonic material in mid-infrared

- Metasurface tuning using “lossless” SLG
- MMs enable graphene characterization in mid-IR

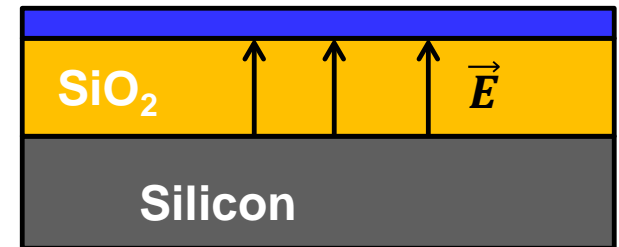


Integration of MMs with Gated SLG



- Back-gating injects carriers into graphene → shifts Fermi energy, changes conductivity
- Graphene's conductivity affects metamaterial's resonances → graphene spectroscopy
- Frequency shift comparable to linewidth → strongly-coupled regime of graphene-MM interaction

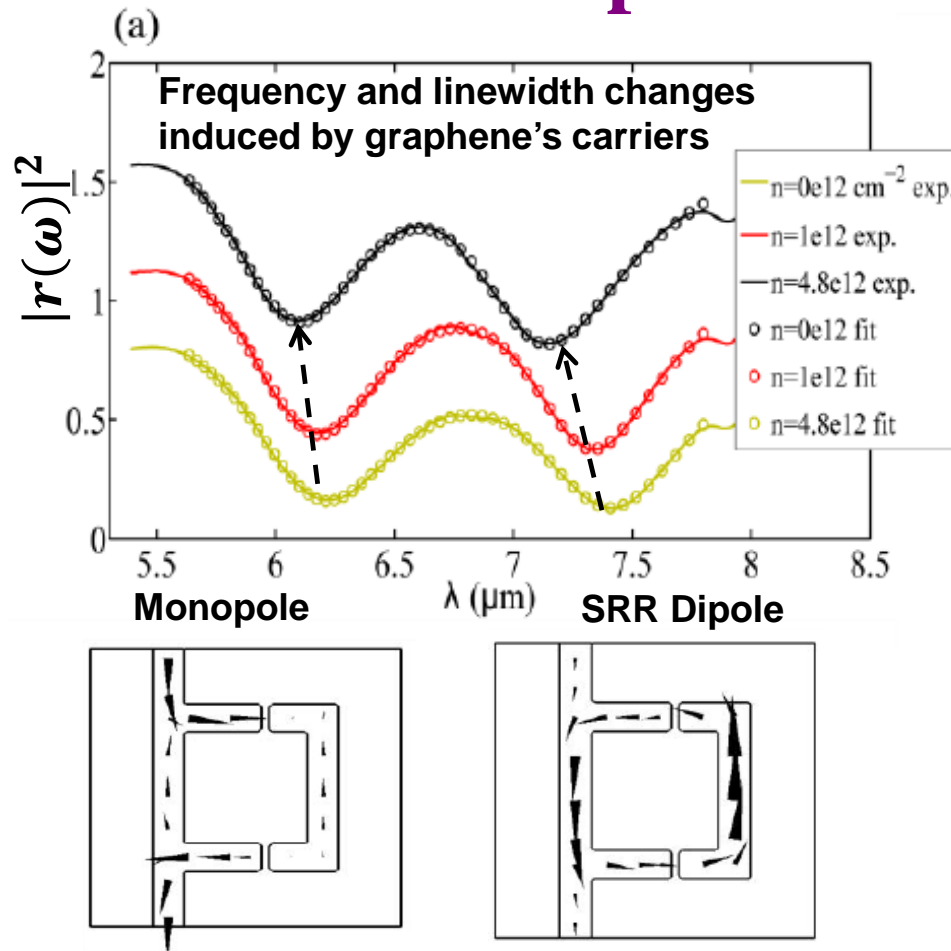
Graphene: free + bound carriers



Antenna arrays: N. K. Emani et. al., Nano Lett. **12**, 5202 (2012);
Y. Yao et. al., NanoLetters **13**, 1257 (2013)

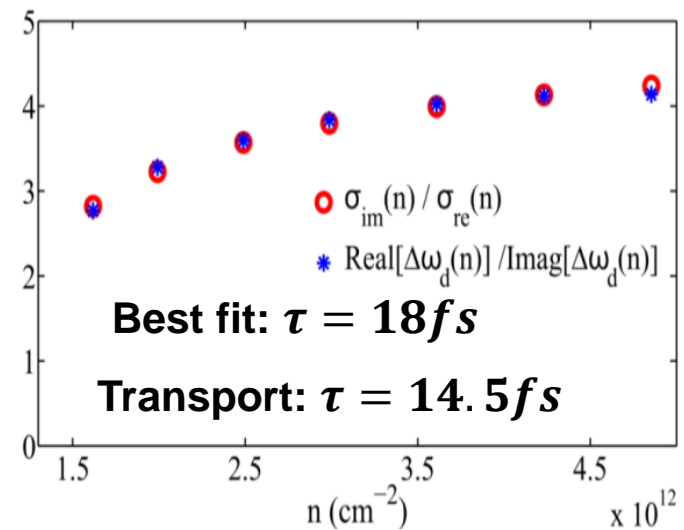


Double-Fano Resonance Fit Used to Extract Graphene's Optical Properties



$$\frac{\text{Re}(\Delta\omega_{m,d})}{\text{Im}(\Delta\omega_{m,d})} = \frac{\text{Im}(\sigma)}{\text{Re}(\sigma)}$$

Calculate Fermi energy E_F and carrier relaxation time τ in the Drude model of graphene conductivity



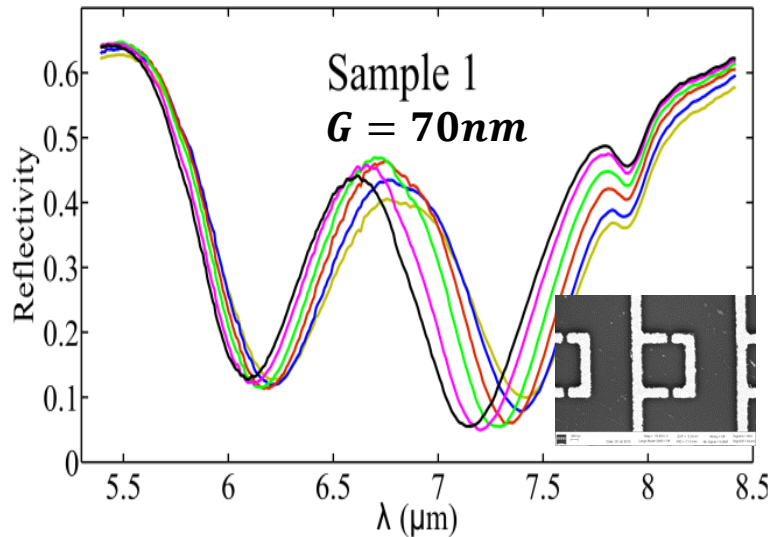
$$r(\omega) = \frac{A_0}{i\omega + 1/\tau_0} + \frac{A_m}{i(\omega - \omega_m) + 1/\tau_m} + \frac{A_d}{i(\omega - \omega_d) + 1/\tau_d}$$

$$\sigma_D = \frac{ie^2}{\pi\hbar} \left\{ \frac{E_F}{\hbar(\omega + i\tau^{-1})} \right\}$$



Amplitude Modulator Based on MM/SLG

Modulate reflectivity around Dirac point by back-gating graphene

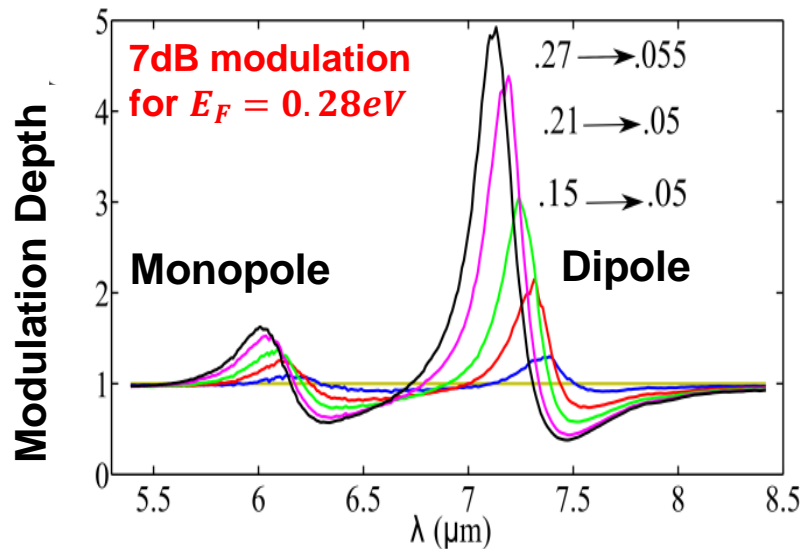


Two properties satisfied by efficient modulators:

- (a) High baseline “on” reflectivity ($E_F = 0$)
- (b) High modulation depth (maximum E_F)

Metamaterials + graphene have both

(c)

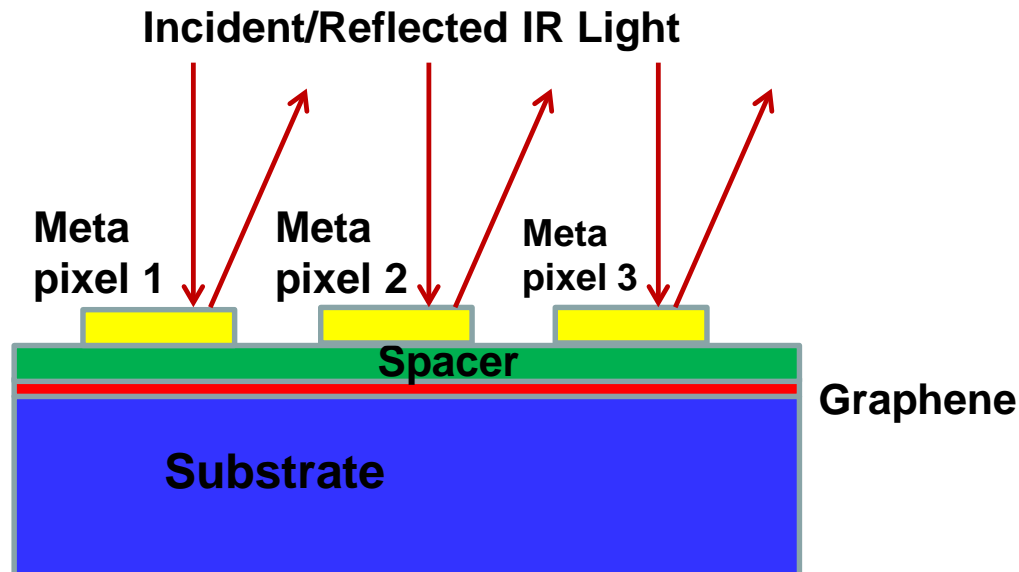
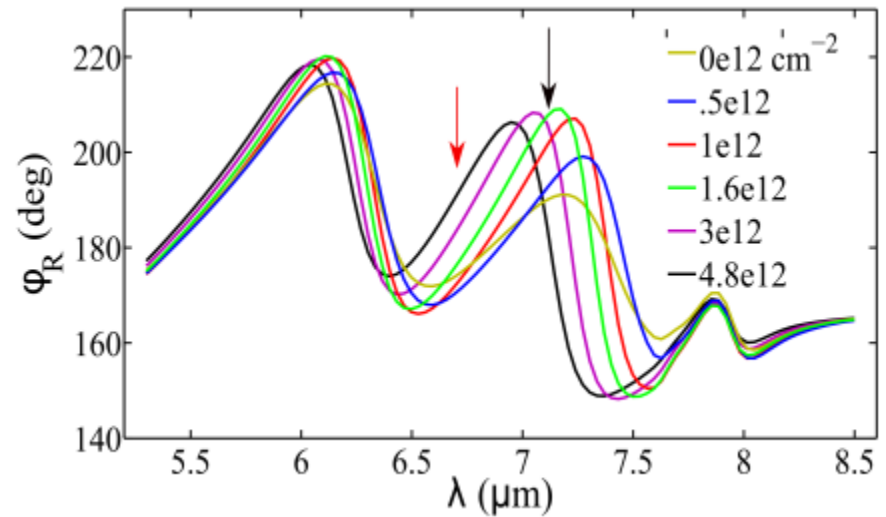
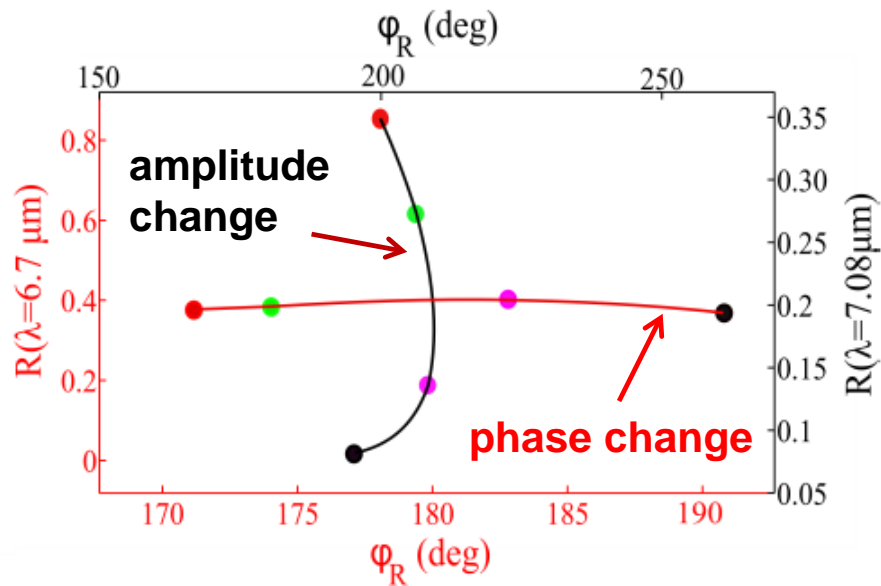


Modulation Depth: $R(\lambda; E_F = 0)/R(\lambda; E_F)$

- 0e12 / 0 V
- .5e12 / -40 V
- 1e12 / -80 V
- 1.6e12 / -130V
- 3e12 / -240 V
- 4.8e12 / -390V

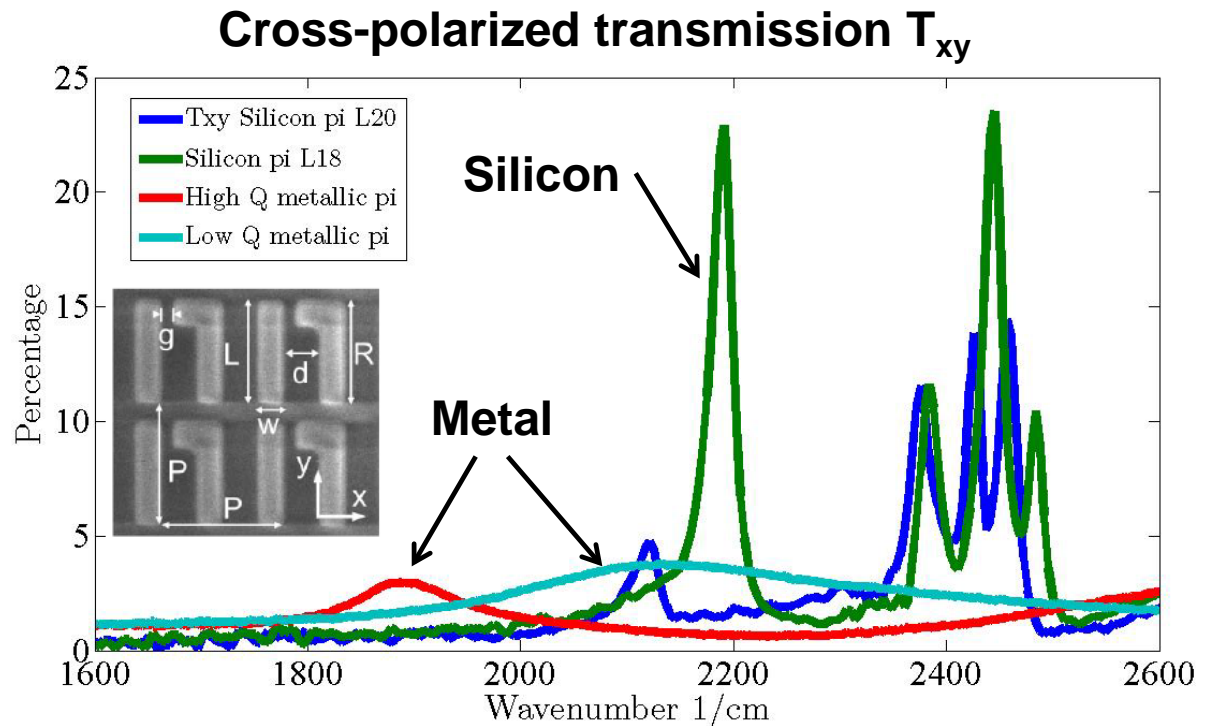
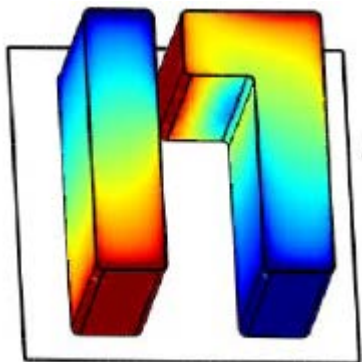
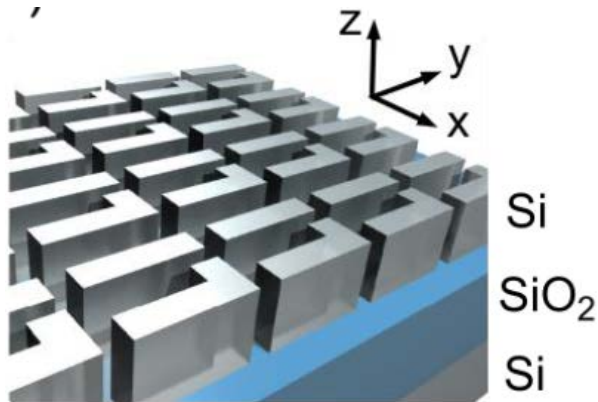


IR Amplitude/Phase Modulator with SLG



- Either phase or amplitude can be electrically modulated
- Independently controlled pixels \rightarrow electrically controllable IR beam steering or modulation or both
- This can be done either in reflection or in transmission

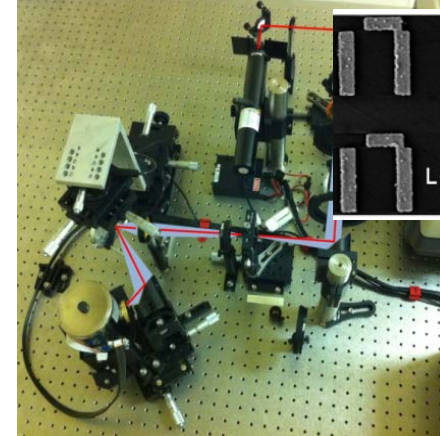
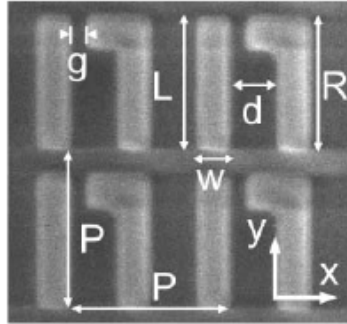
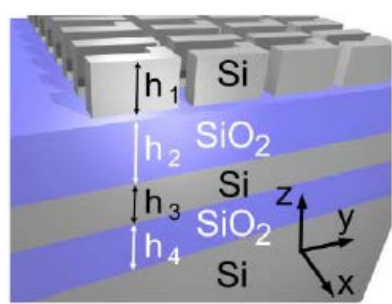
All-Dielectric Fano-Resonant 2D Chiral Metasurfaces: Order of Magnitude Higher Q Than Similar Metallic Metasurfaces



C. Wu et. al., "Spectrally Selective Chiral Silicon Metasurfaces Based on Infrared Fano Resonances", Nature Communications (in press, 2014)



High-Q Fano Resonance in Dielectric MSs

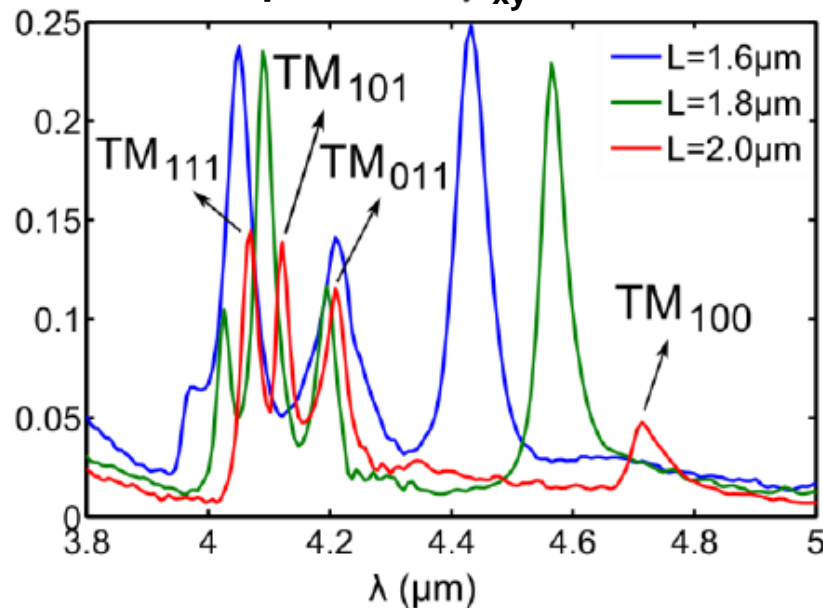


near-field FTIR
spectroscopy using
high-NA (≈ 0.14)
obliquely incident IR

beam focused to
 $W=200\mu\text{m}$

$P = 2.4\mu\text{m}$, $w = 500\text{nm}$, $h_1 = h_3 = 1.2\mu\text{m}$
 $g = 200\text{nm}$, $d = 700\text{nm}$, $h_2 = h_4 = 1.6\mu\text{m}$
 $R = 2\mu\text{m}$, $L = 1.6 - 2\mu\text{m}$

Experiment, T_{xy}



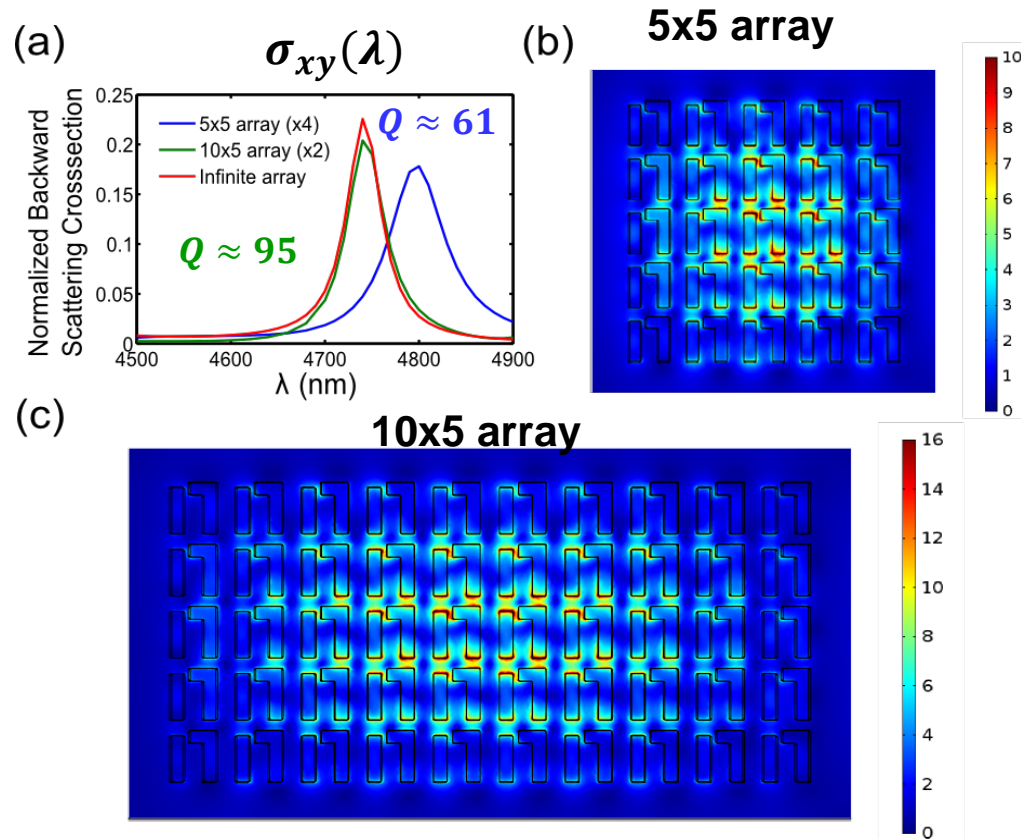
Dark mode

Nanorod length

	$L = 2\mu\text{m}$	$L = 1.8\mu\text{m}$	$L = 1.6\mu\text{m}$
TM ₁₀₀	$Q = 75.7$ $\lambda = 4.71\mu\text{m}$	$Q = 94.3$ $\lambda = 4.57\mu\text{m}$	$Q = 73.9$ $\lambda = 4.43\mu\text{m}$
TM ₀₁₁	$Q = 113.3$ $\lambda = 4.21\mu\text{m}$	$Q = 100$ $\lambda = 4.2\mu\text{m}$	$Q = 52.9$ $\lambda = 4.21\mu\text{m}$
TM ₁₀₁	$Q = 113.7$ $\lambda = 4.12\mu\text{m}$	$Q = 111.7$ $\lambda = 4.09\mu\text{m}$	$Q = 76.1$ $\lambda = 4.05\mu\text{m}$
TM ₁₁₁	$Q = 116.9$ $\lambda = 4.07\mu\text{m}$	$Q = 127.5$ $\lambda = 4.03\mu\text{m}$	$Q = 98.4$ $\lambda = 3.97\mu\text{m}$



Collective Effects In Metasurfaces



Each unit cell interacts with 2-3 neighbors on each side horizontally and about 1 cell on each side vertically \rightarrow short-range interaction

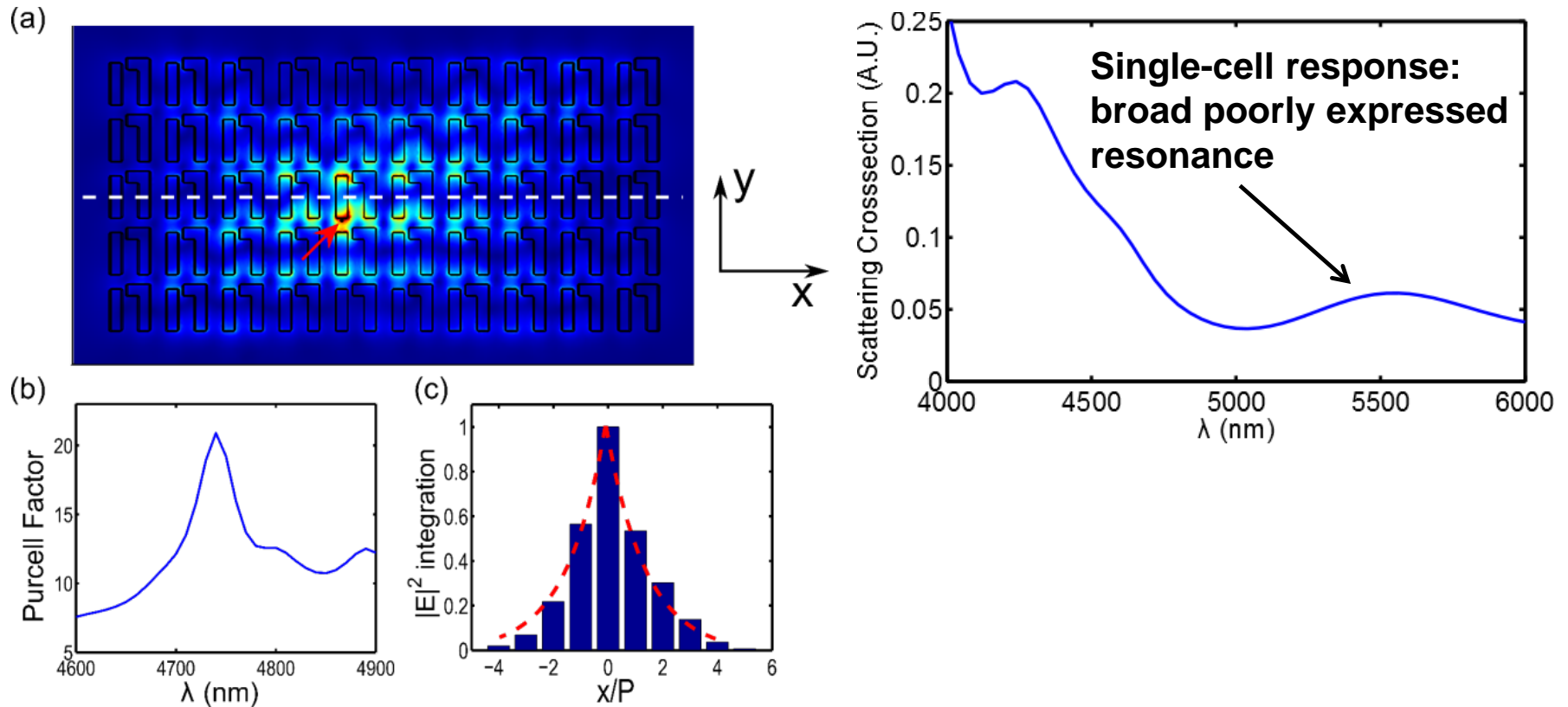
Pixels as small as $6\lambda \times 3\lambda$ have identical $Q \approx 95$ as infinite arrays

Pixels as small as $3\lambda \times 3\lambda$ have $Q \approx 61 \rightarrow$ number of peripheral cells exceeds the number of central cells

- Near-neighbor interactions are important in collective meta-surfaces, but not nearly as much as in 2D photonic crystals \rightarrow distinct concept
- A 2D PhC with $Q \approx 100$ operating at $\lambda = 5\mu m$ would have to be rather large ($0.5mm \times 0.5mm$), and would require a collimated beam with $\delta\theta = 0.6^\circ$



Importance of Close-Neighbor Interactions



Near-field excitation reveals a narrow-band peak in the photonic density of states

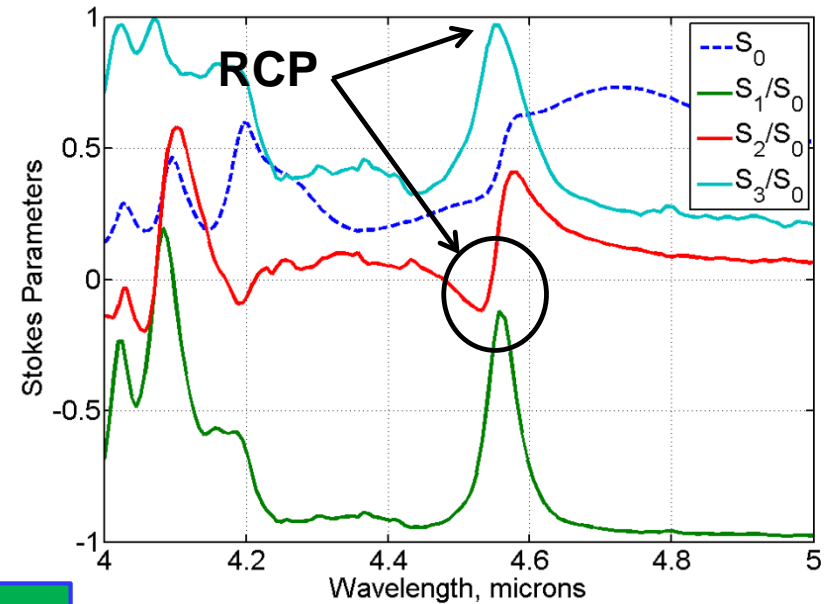
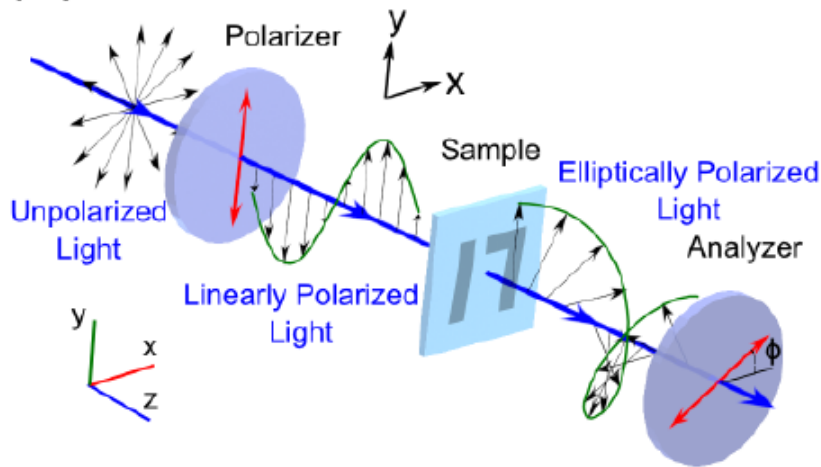
Collective close-neighbor interactions persist over periods → each unit cell must have at least 2 nearest neighbors on each side horizontally

Conceptually different from PhC → “almost-collective” metasurface



LP → CP: Stokes Parameter Extraction

Rotating analyzer Stokes polarimetry



- LP → CP conversion by 1 micron thick MS with high efficiency (50%) at normal incidence
- Experimentally measured quality factor $Q \approx 95$
- Close to 100% Degree of Circular Polarization

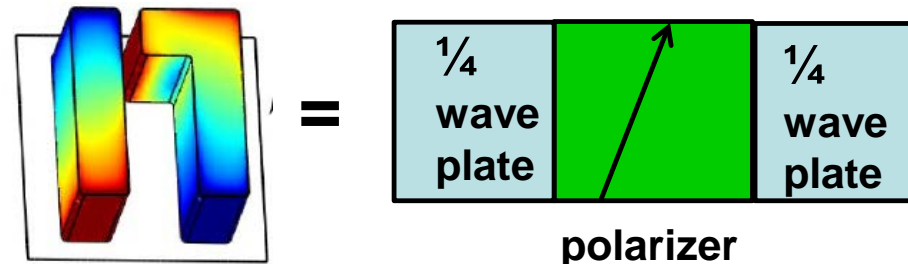
$$S_1 = I_x - I_y, S_2 = I_{45^\circ} - I_{-45^\circ}$$

$$S_0 = I_x + I_y, |S_3| = |I_{RCP} - I_{LCP}|$$

How does LP → CP conversion work?

How is it different from regular birefringence or 3D chiral structures?

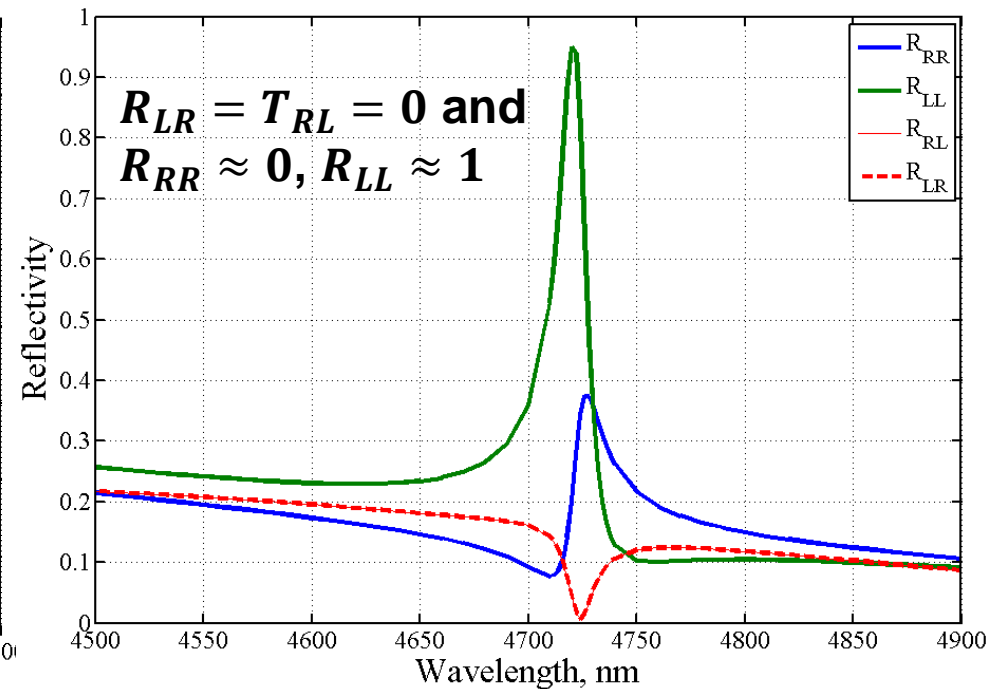
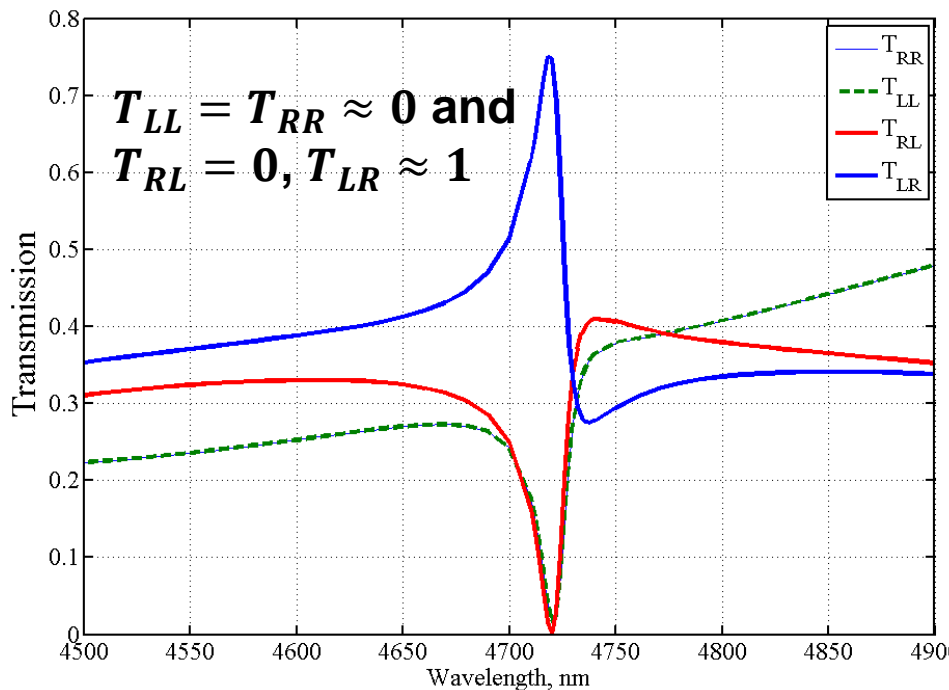
Can one use chiral MS for developing a CP thermal emitter?





Super-Chiral Metasurfaces

Objective: $T_{RR} + T_{RL} \ll T_{LL} + T_{LR} \rightarrow$ high Degree of Circular Polarization



Only RCP gets transmitted. And when it does, it gets flipped into LCP!

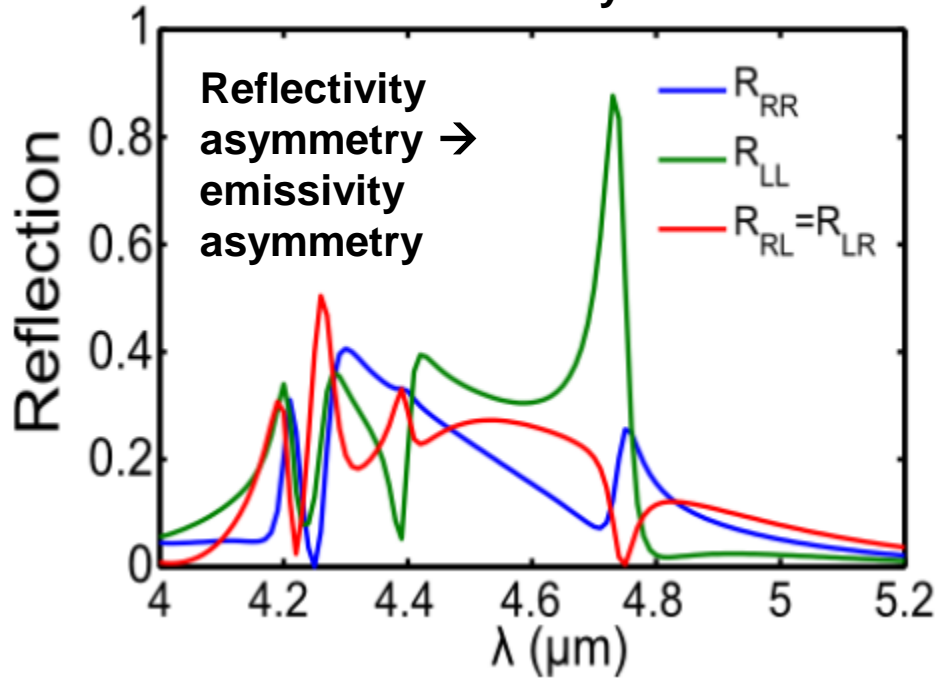
**All of LCP gets reflected...as LCP
 \rightarrow Super-Chiral Mirror!**

- The effect does not require (a) dissipation, (b) substrate/air mismatch, (c) non-normal incidence \rightarrow [$\frac{1}{4} \lambda$ plate + polarizer + $\frac{1}{4} \lambda$ plate] $1 \mu m$ thick!
- It requires finite thickness ($h \approx \lambda/4 \rightarrow$ impossible with noble metals), periodicity, and bi-anisotropy ($M_z \propto \kappa E_y$)

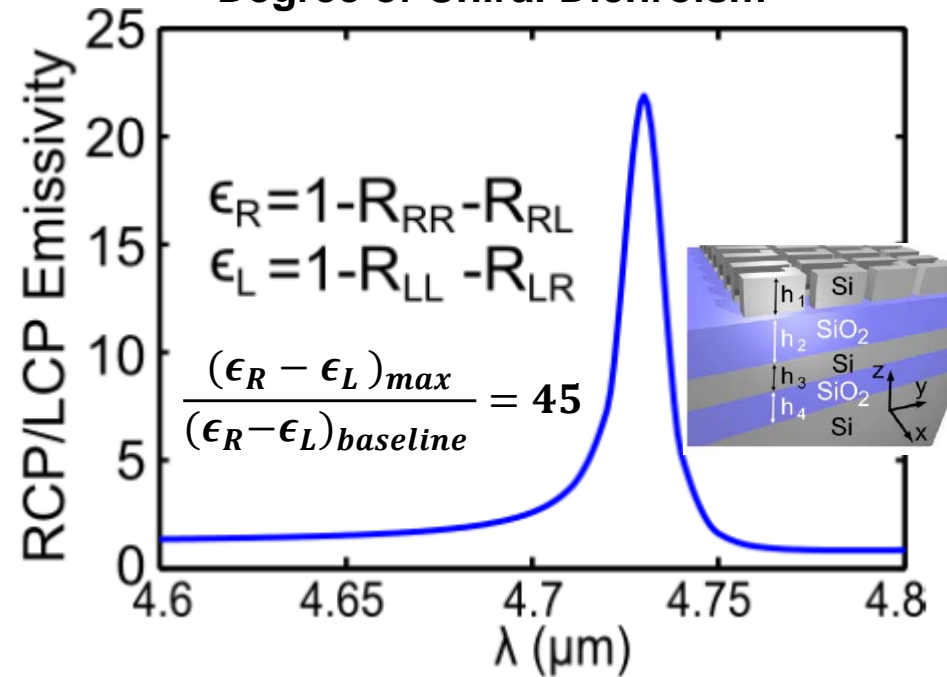


Spectrally Selective CP Thermal Emission

RCP/LCP Reflectivity Matrix



Degree of Chiral Dichroism

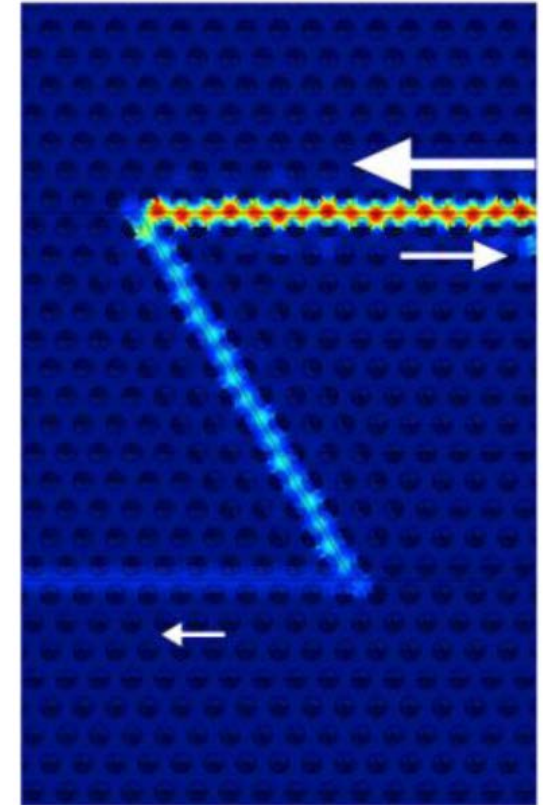
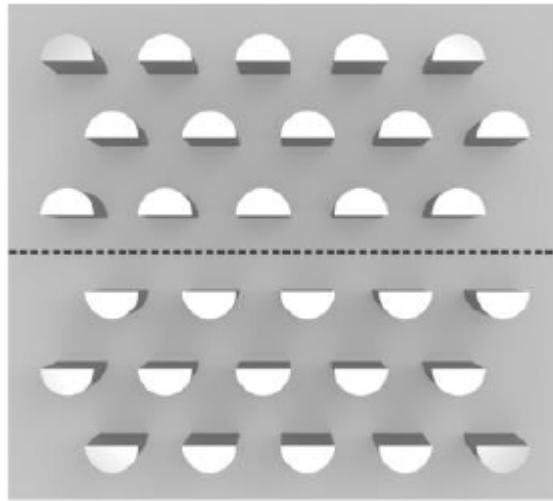
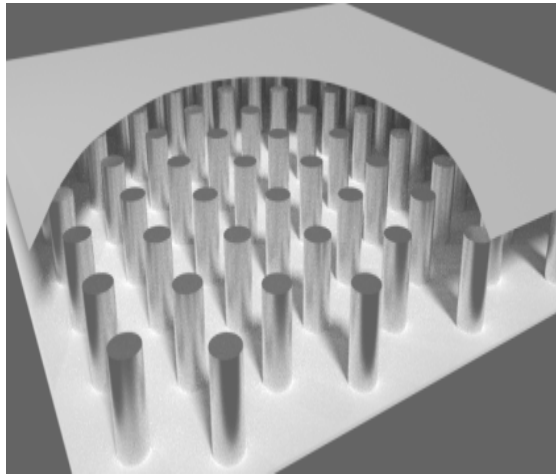


Infrared ID Tags Applications: Unique Spectral/Polarization Signatures!

- $\sigma_{FWHM} \approx 25\text{nm}$: more than 12 CP emission lines separated by $6 \cdot \sigma_{FWHM}$ inside the $\lambda = 3 - 5\mu\text{m}$ IR transparency window
- The entire scene emits thermal IR, but it is not circularly polarized \rightarrow unique opportunities for IR Identification Tags
- Each line can be RCP, LCP, or un-polarized: $3^{12} = 530,000$ unique IR identification tags with unique spectral/polarization signatures



Avoiding Reflections Using Photonic Topological Protection

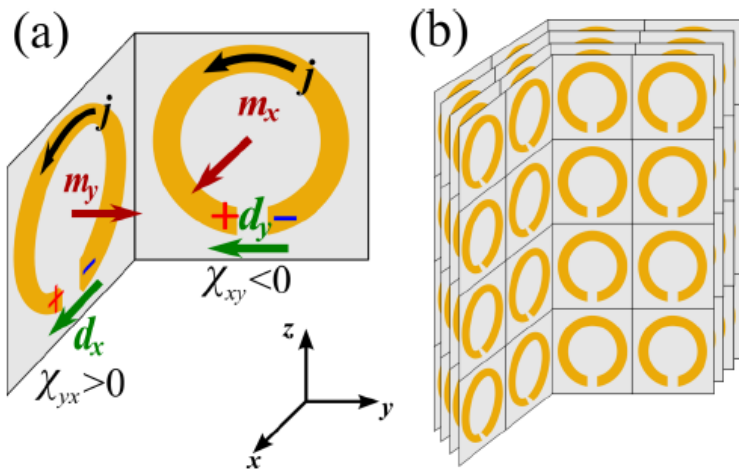


Property of a scalar wave equation: any obstacle/bend on the scale of one wavelength is going to cause reflections of the microwaves!

This is true for either bulk or surface waves

•There is a precedent of suppressed reflections in physics: an electron with spin- $\frac{1}{2}$ and strong spin-orbit coupling propagates without scattering!

Emulating Electron Spins and Topological Insulators Using Bi-anisotropic Metamaterials



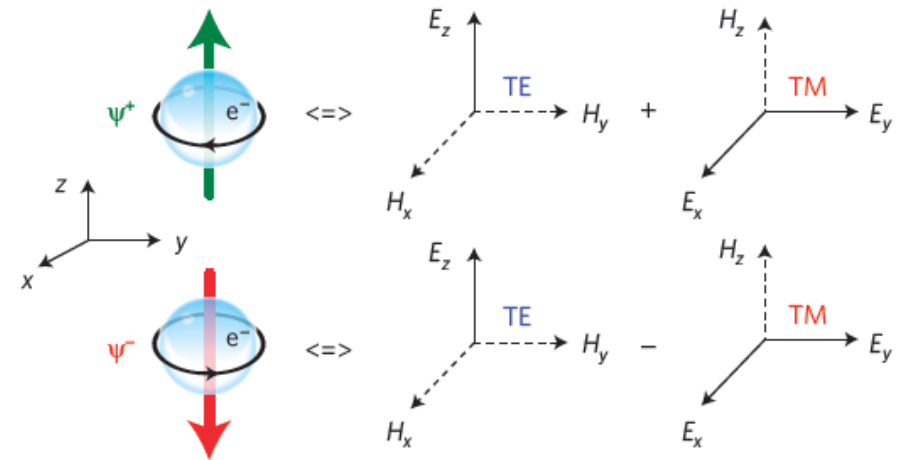
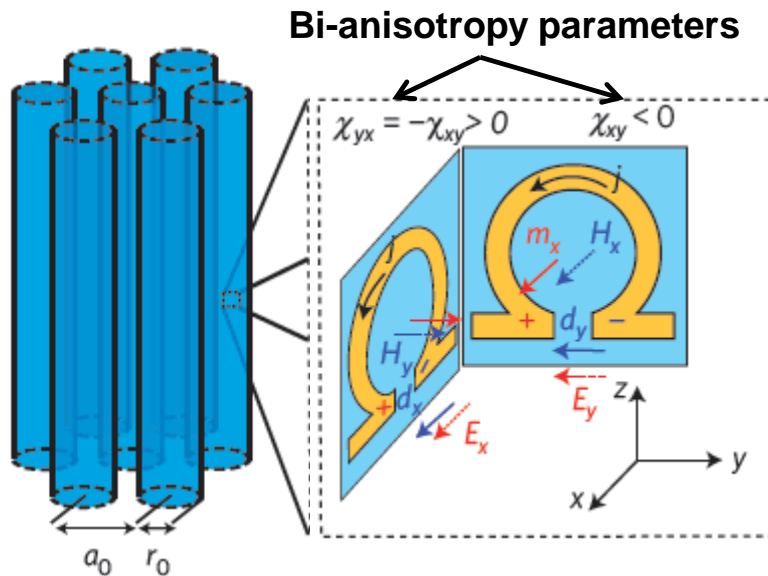
$$\vec{\nabla} \times \vec{E} = +\frac{i\omega}{c} \left(\overline{\overline{\mu}} \cdot \vec{H} + \overline{\overline{\zeta}} \cdot \vec{E} \right)$$

$$\vec{\nabla} \times \vec{H} = -\frac{i\omega}{c} \left(\overline{\overline{\xi}} \cdot \vec{H} + \overline{\overline{\epsilon}} \cdot \vec{E} \right)$$

Bi-anisotropy requires breaking mirror reflection symmetry



From Metamaterial to Meta-Crystal



2-D PhMC: Photonic Crystal comprised of metamaterial inclusions

$$\psi^\pm(x_\perp; \mathbf{q}) = E_z(x_\perp; \mathbf{q}) \pm H_z(x_\perp; \mathbf{q})$$

$$\left(k_0^2 \epsilon_{zz} + \nabla_\perp \frac{1}{\mu_\perp} \nabla_\perp \right) \psi^\pm = \pm \left[\nabla_\perp \left(\frac{-i\chi_{xy}}{\epsilon_\perp \mu_\perp} \right) \times \nabla_\perp \psi^\pm \right]_z$$

- Photonic equivalents of spin-up and spin-down electron states
- Requires spin-degenerate metamaterials: $\epsilon_{zz} = \mu_{zz}$, $\epsilon_\perp = \mu_\perp$
- Exact emulation of Kane-Mele Hamiltonian of graphene TIs



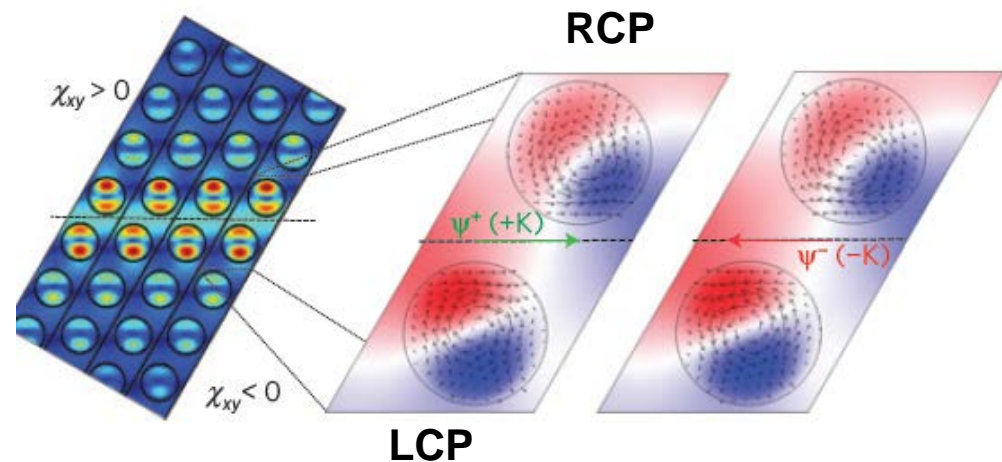
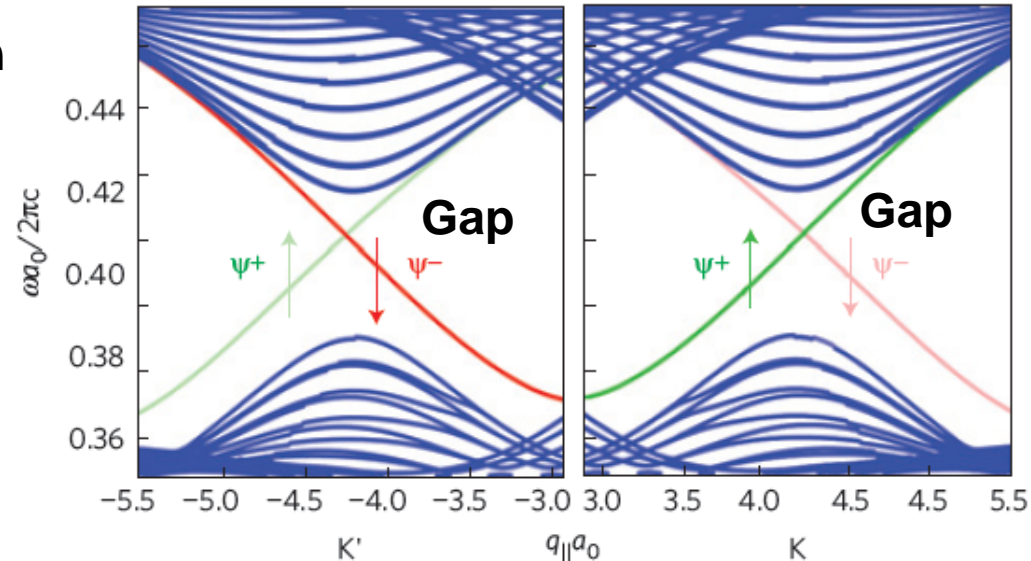
Interfaces: Edge States of PTIs

Interfaces between PTIs (e.g. between $\chi_1 > 0$ and $\chi_2 < 0$) support one-way spin-degenerate states!

“Spins” don’t scatter into each other as long as the materials are spin-degenerate: $\epsilon_{zz} = \mu_{zz}$, $\epsilon_{\perp} = \mu_{\perp} \rightarrow$ restricted topological protection

Spin degree of freedom \rightarrow relative phase between E_z and H_z

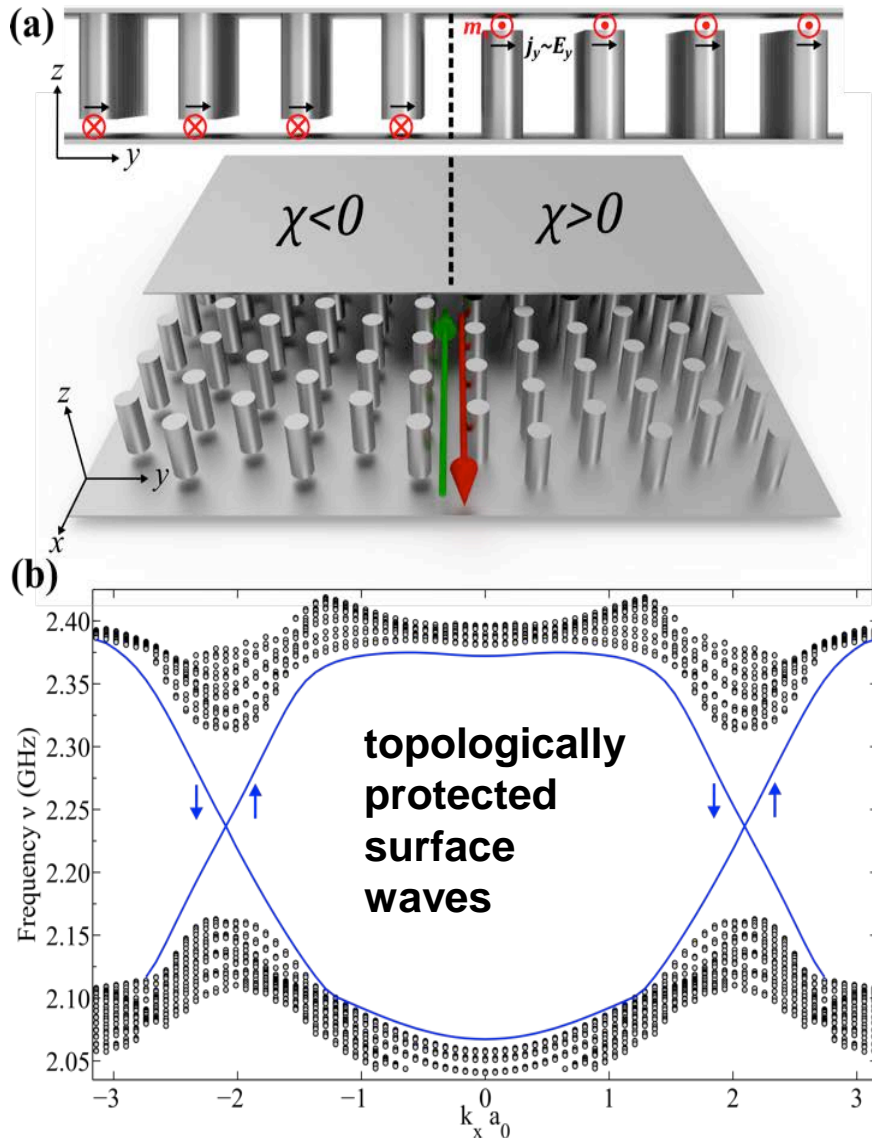
Orbital degree of freedom \rightarrow CP at K point of Brillouin zone



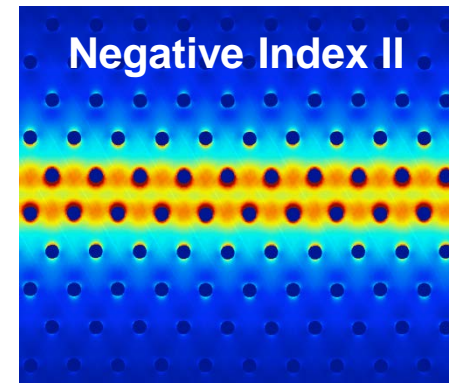
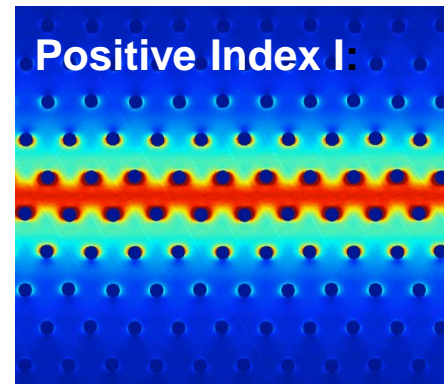


From Meta-Crystals to Meso-MMs

Topological Interface



Bi-anisotropic Meta-Waveguide (BMW) \rightarrow simplified version of PTIs emulates spin-orbit coupling



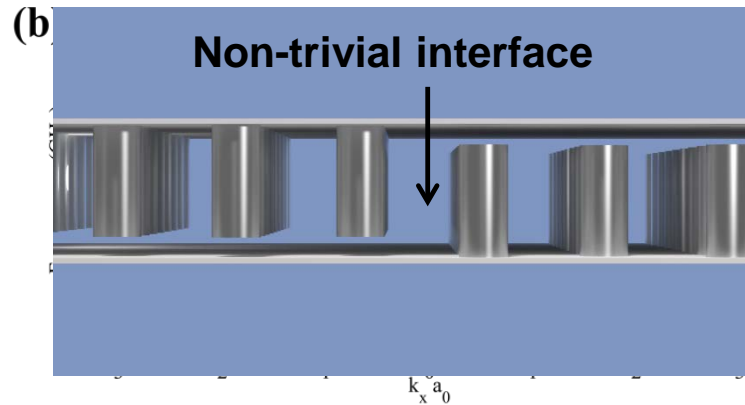
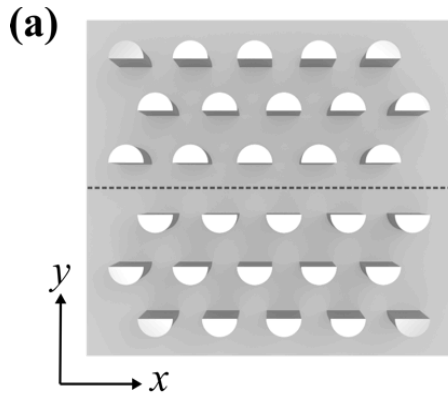
Spin-polarized photon flow: two spin-up states moving forward, two spin-down states moving backward

Topological protection of edge states against backscatter

Fundamentally different from Tamm states!

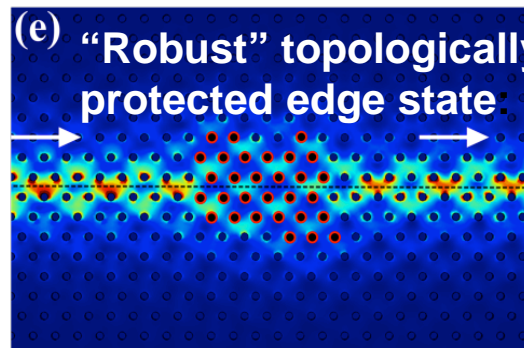
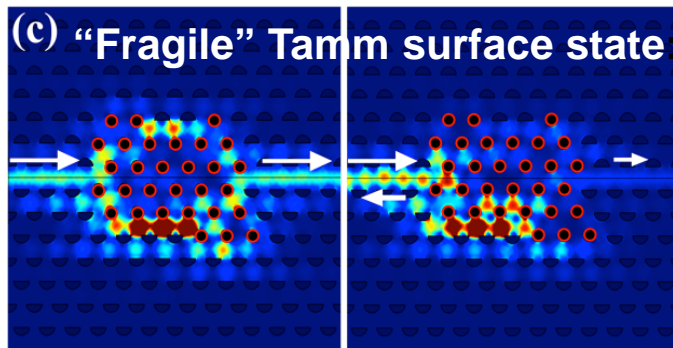


Tamm States vs Topologically Protected Edge States: Disorder Sensitivity

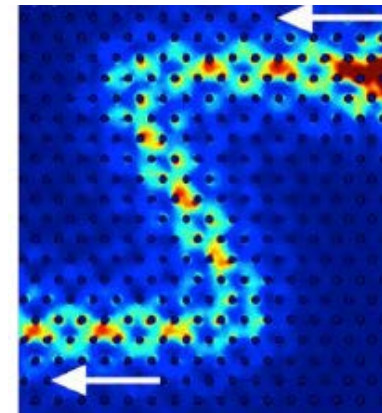
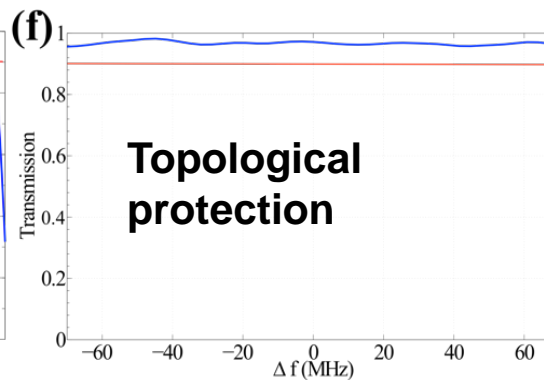
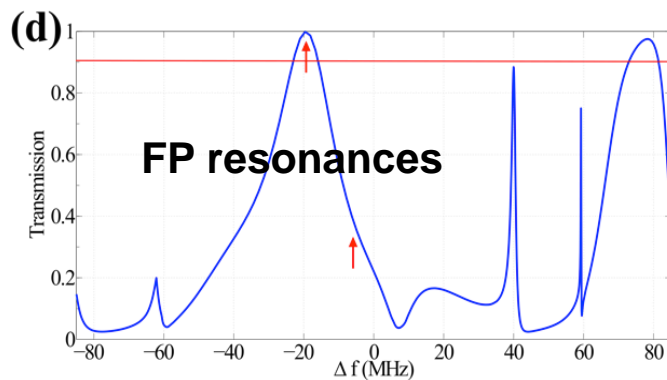


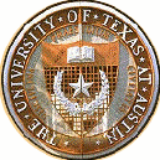
“Cavity” placed along the interface \rightarrow transmission depends on the nature of edge state:

(1) Tamm state \rightarrow small transmission interrupted by Fabry-Perot resonances

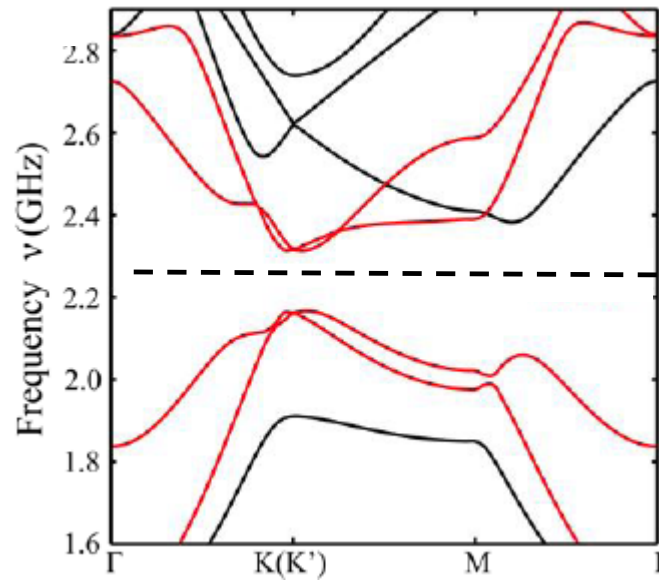
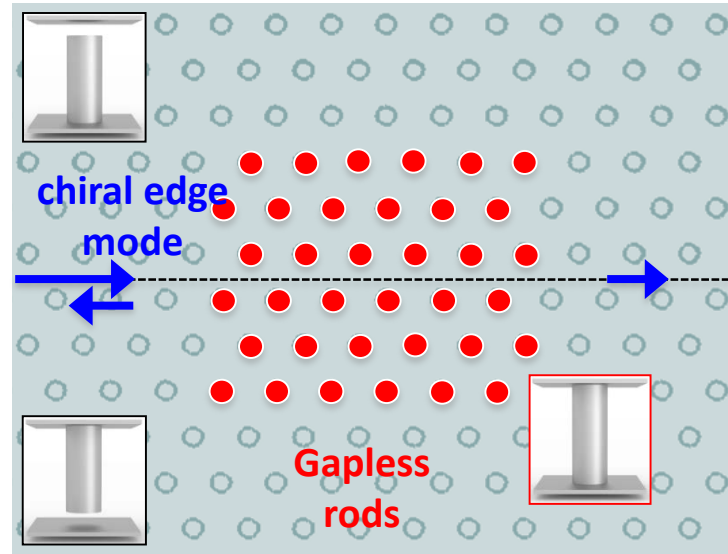


(2) Topologically protected edge state \rightarrow nearly perfect transmission \rightarrow guide waves around corners

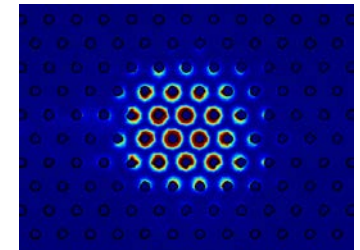




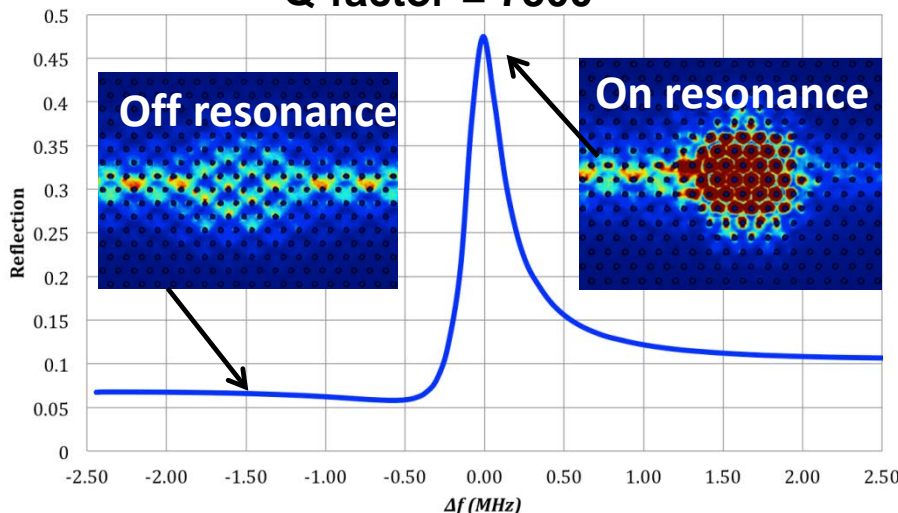
Breaking topological protection



Resonant magnetic impurity inside topological bandgap



Q-factor = 7500



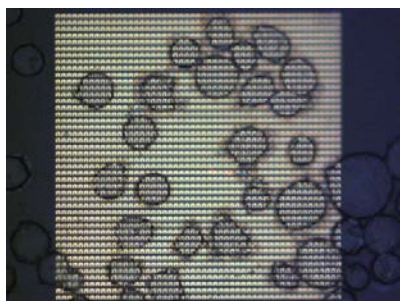
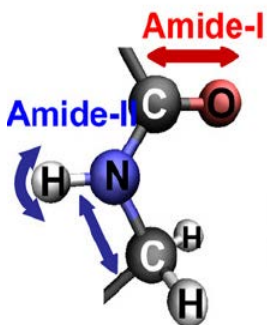
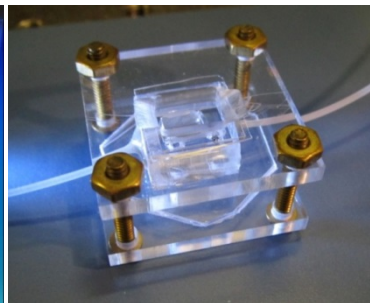
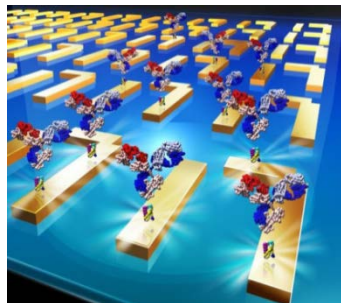
Cavity eigenmode couples $\uparrow\downarrow$ spin states \rightarrow resonant backscattering is allowed by spin-flipping!

Two-mode theory collapses in the presence of third mode!

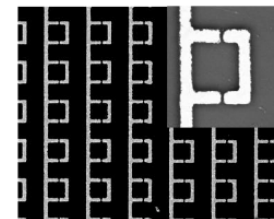
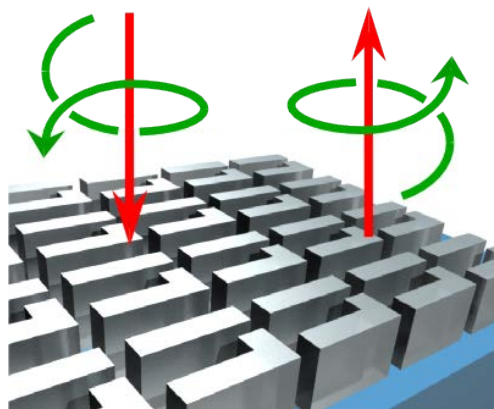
Nonlinearities also break topological protection \rightarrow emulation of many-body effects in CM



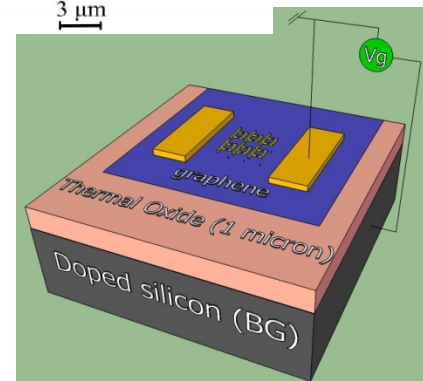
What Can Metamaterials Do For You: Applications Time!



All-dielectric super-chiral metasurfaces with $Q > 100$



3 μm



C. Wu et.al., Nature Materials **11**, 69 (2012) \rightarrow surface-enhanced IR spectroscopy of protein monolayer; microfluidic integration for cell identification in blood (CTCs)

C. Wu et.al., Nature Comm. (in press) \rightarrow engineering of thermal/quantum emission \rightarrow sources of CP radiation across EM spectrum

S. H. Mousavi et. al., NL **13**, 1111 (2013) \rightarrow integration of SLG with metamaterials \rightarrow agile IR modulators, beam steering.



Acknowledgements



Postdocs/Staff:

Simeon Trendafilov

PhD Students

S. Austin Yi

Nihal Arju

Hossein Moussavi

Nima Dabidian

Chih-Hui Wu

Collaborators:

Igal Brener (SNL)

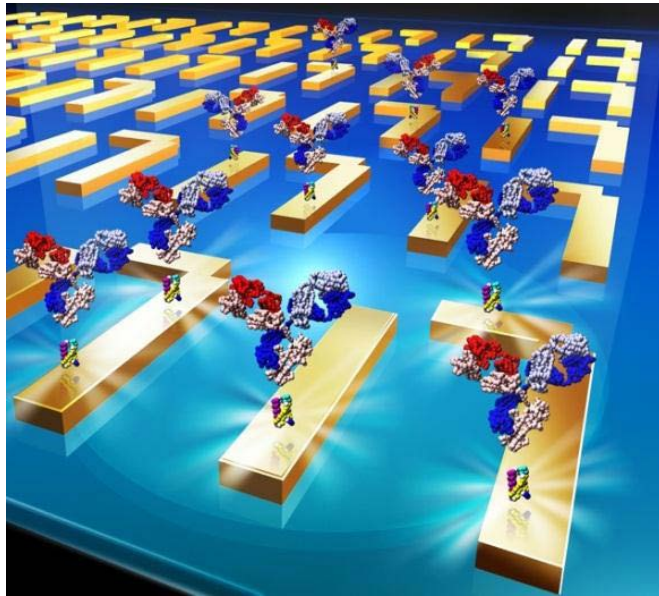
Rod Ruoff (UT)



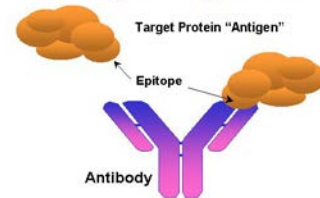


Additional Slides

Novel platform for bio-sensing and molecular fingerprinting: Metasurface Enhanced Infrared Reflection Spectroscopy → MEIRS



Antibody-Antigen Binding

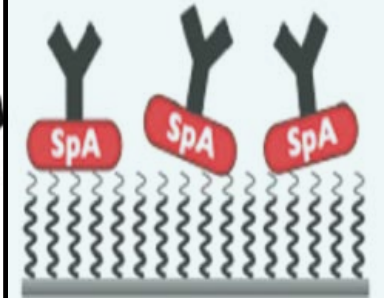


substrate

c) partially oriented IgG on randomly-oriented (physisorbed) SpA



d) well-oriented IgG on oriented SpA (tyrosinase-catalyzed)

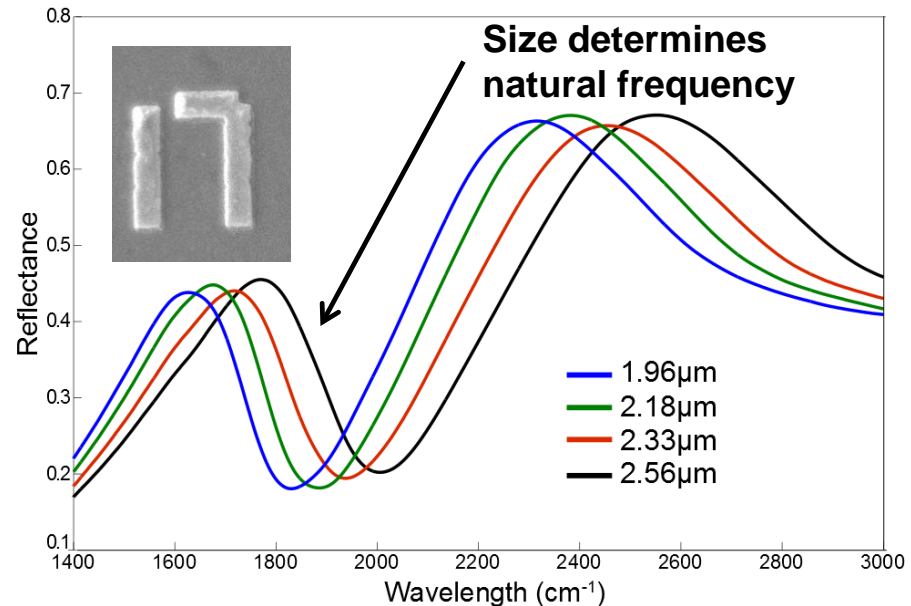
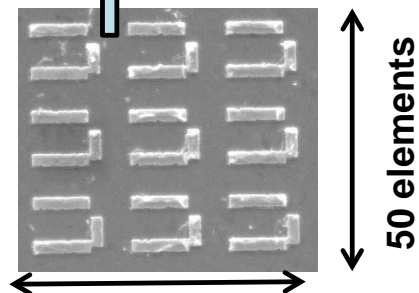
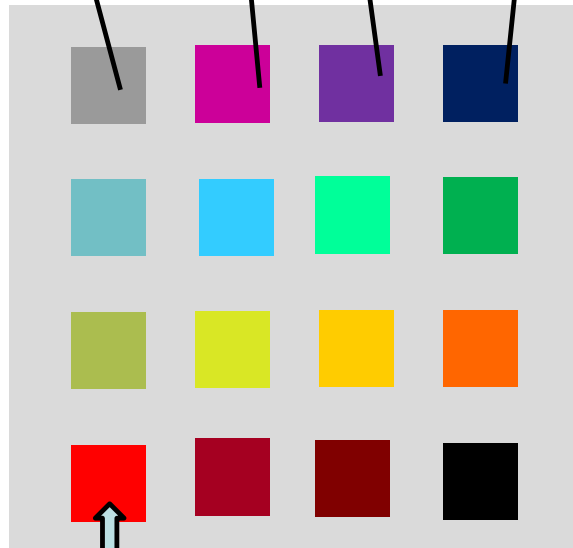
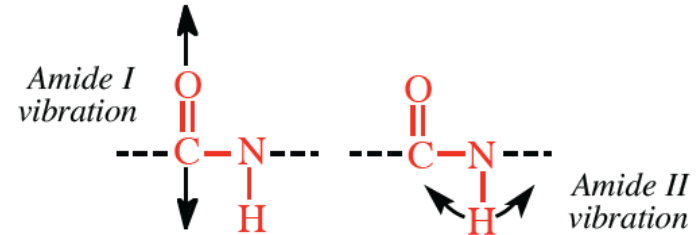
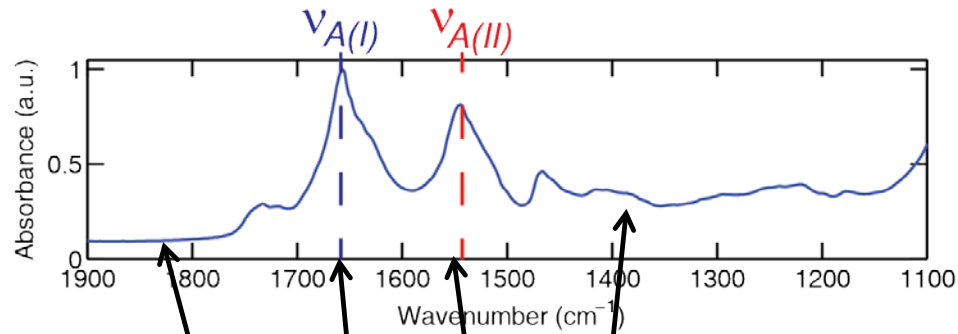


Chihhui Wu et.al., Nature Materials
11, 69 (2012)

Objective: better biosensor by improving the orientation of binding proteins and antibodies → higher binding capacity



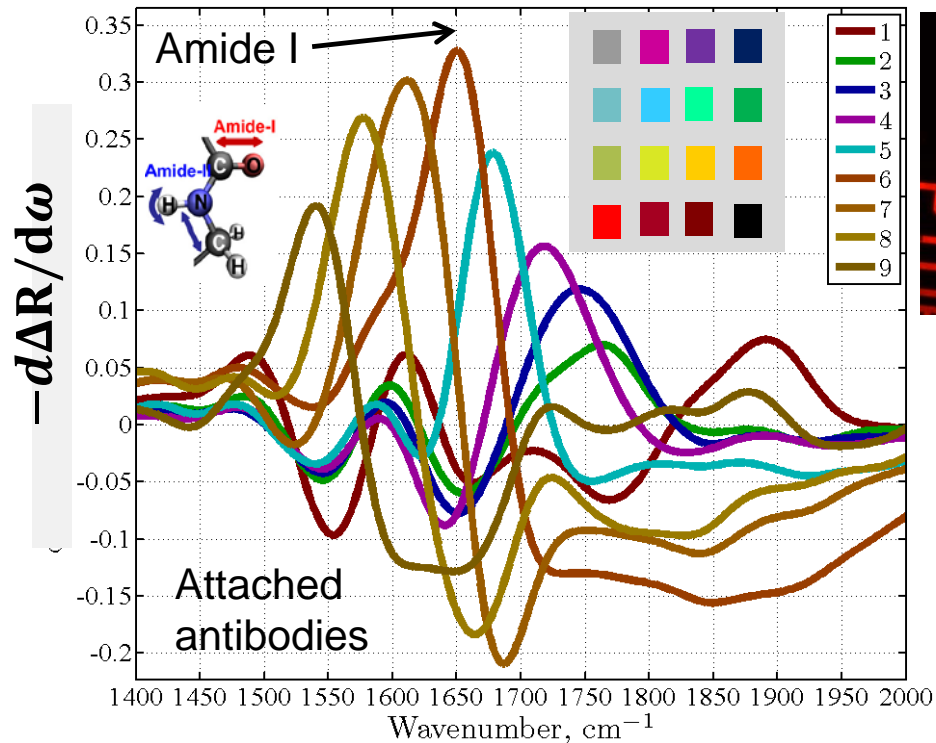
Meta-Pixels Mosaic Tuned to Fingerprints



- **Pixels' resonance frequencies** can be swept across vibrational resonances
- **Resonant and non-resonant pixels** \rightarrow additional data points for bio-sensing



How sensitive is MEIRS: Comparison with Fluorescence Measurements



Fluorescently tagged antibodies before washing



Attached antibodies (after washing): fluorescence not observed under microscope

$\Delta R(\omega)$: Difference spectrum (with protein – bare) \rightarrow peaks at the MM resonance

- Single monolayers of fluorescently tagged antibodies are difficult to detect using unspecialized microscopes
- Metasurface-enhanced infrared spectroscopy (MEIRS) enables the detection of antibody monolayers \rightarrow strongest signal when metasurface resonance is matched to vibrational resonance of the protein (e.g., Amide I)
- **Advantageous to avoid exogenous labels for tagging**

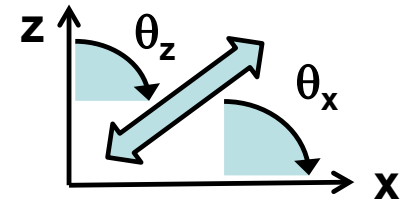


Interaction of Anisotropic and Oriented Proteins with Metasurfaces



$$T_{ij} = N^{-1} \sum_{k=1}^N \cos \theta_i^{\{k\}} \times \cos \theta_j^{\{k\}}$$

orientation tensor: C=O bond
with respect to Cartesian axes

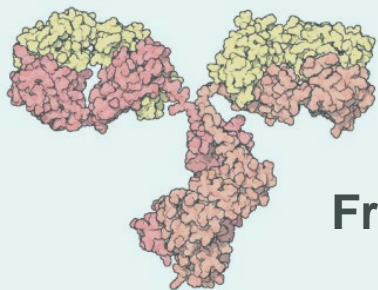


$$T_{ij} = (1/3)\delta_{ij}$$

for isotropic
proteins

$$\varepsilon_p(\omega) = \varepsilon_\infty + \sum_m \frac{A_m T_{zz}}{\omega - \omega_m - i\gamma_m}$$

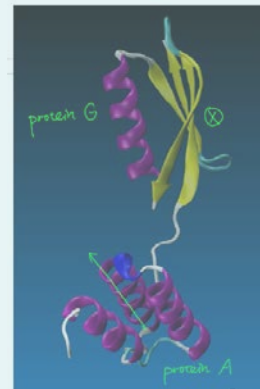
Orientation of anisotropic proteins detected by surface-enhanced spectroscopy



Isotropic
IgG protein

From Protein Data Base

$$T_{ij}^{\text{IgG}} = (0.29; 0.32; 0.39)$$



$$T_{ij}^{\text{A/G}} = (0.14; 0.22; 0.63)$$

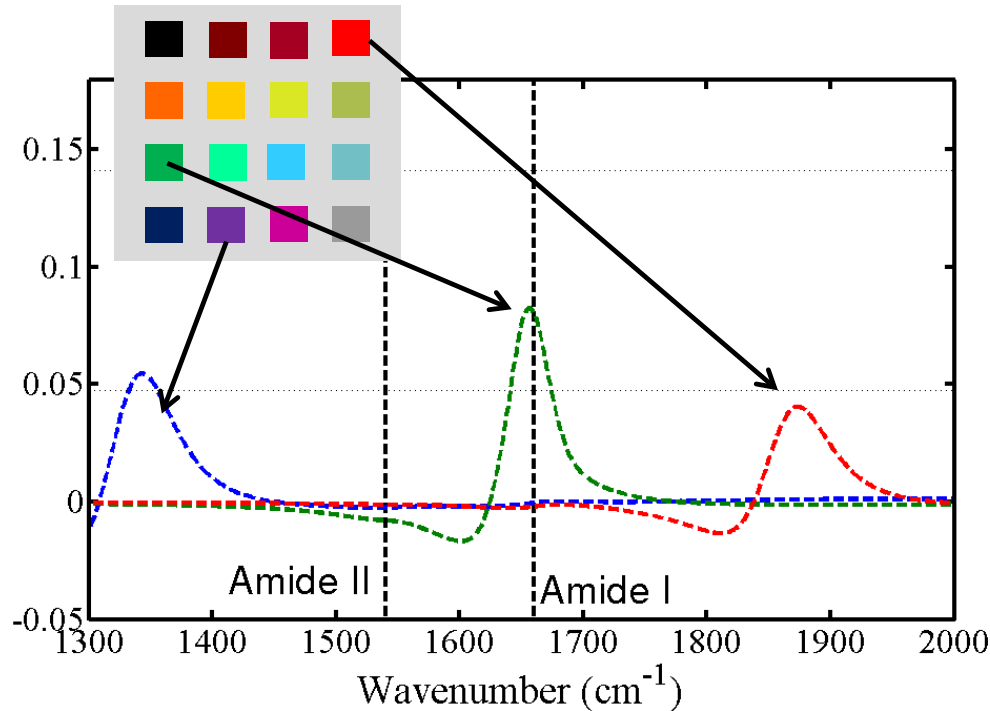
Anisotropic
protein A/G



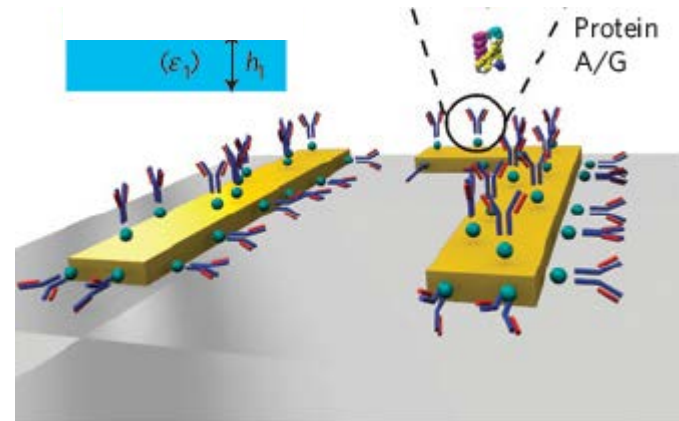
MEIRS determines protein layer compositions

mono-layer: dash

Differential Reflectivity



Binding of A/G monolayer of thickness $h_1=2.7\text{nm}$ to three FRAMM pixels (blue, green, red)



C. Wu et.al., Nature Materials **11**, 69 (2012)

$$\epsilon_p(\omega) = \epsilon_\infty +$$

$$\sum_m \frac{A_m T_{zz}}{\omega - \omega_m - i\gamma_m}$$



Non-resonant **blue** pixel is not vibration sensitive → SPR-like thickness measurement



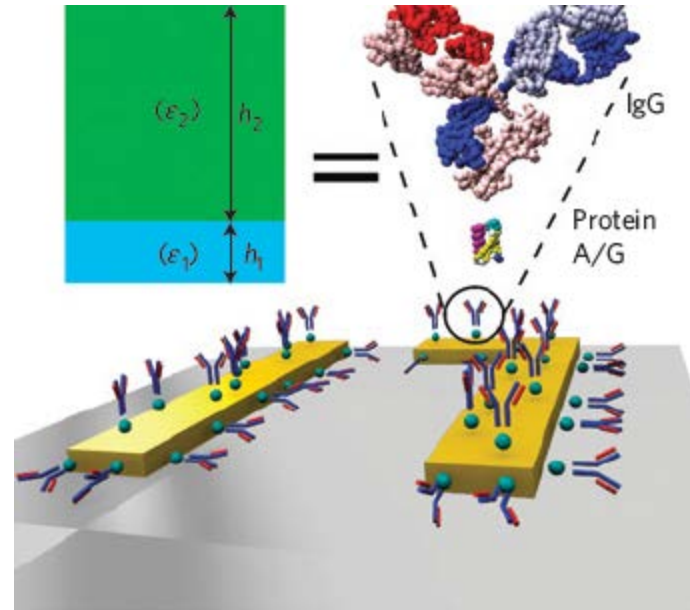
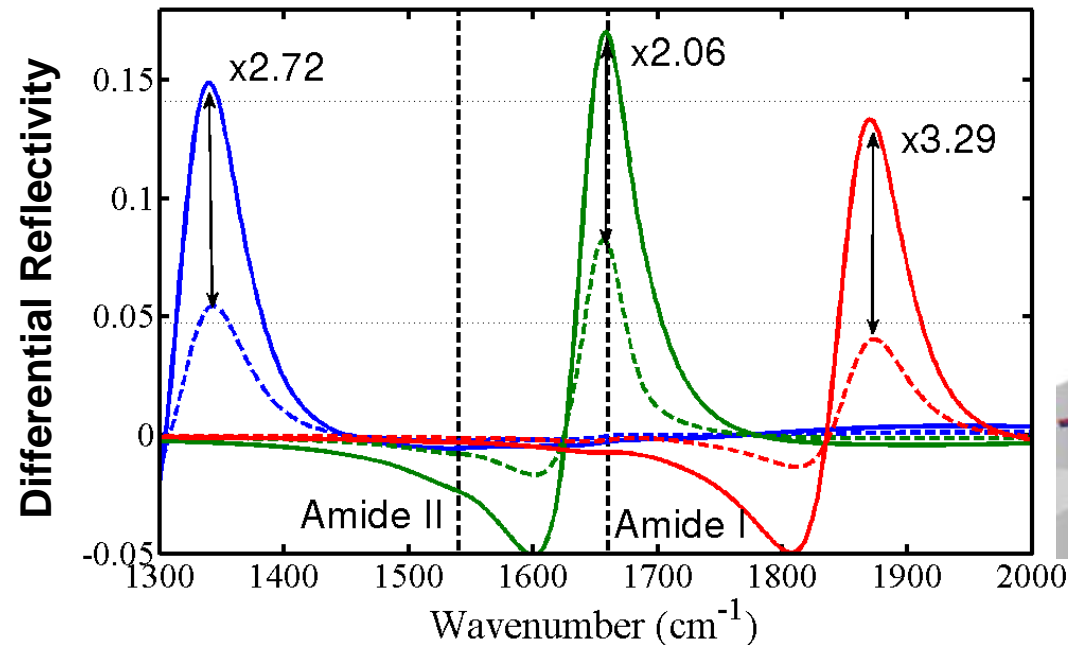
Resonant **green** pixel is vibration/orientation sensitive → orientation of A/G on the surface



MEIRS determine protein layer compositions

mono-layer: dash
bi-layer: solid

IgG monolayer of height $h_2 = 5.1\text{nm}$ binds to A/G
monolayer of height $h_1 = 2.7\text{nm} \rightarrow (h_2 + h_1)/h_1 = 2.9$



$$\varepsilon_p(\omega) = \varepsilon_\infty + \sum_m \frac{A_m T_{zz}}{\omega - \omega_m - i\gamma_m}$$



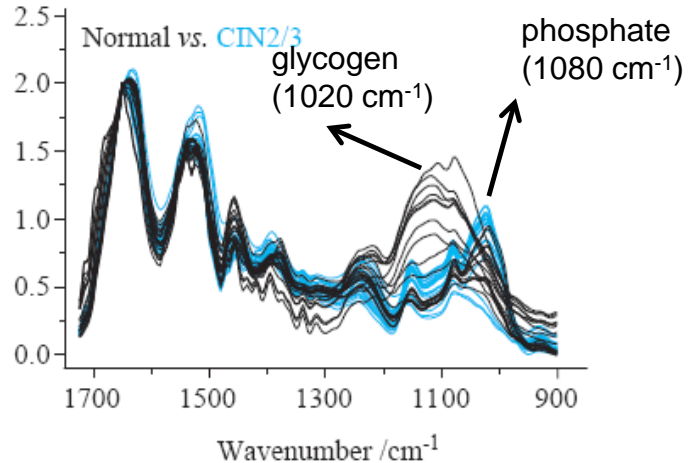
Non-resonant **blue** pixel is not vibration sensitive → SPR-like thickness measurement



Resonant **green** pixel is vibration/orientation sensitive → orientation of A/G on the surface



Where do we go from here: From Proteins to Cells to Diagnostics



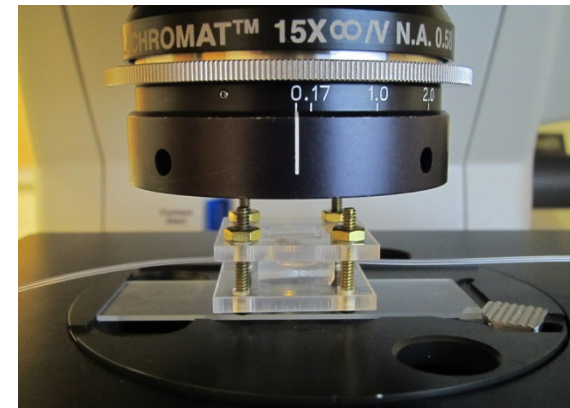
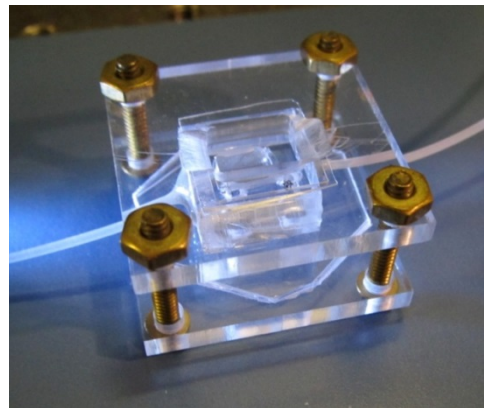
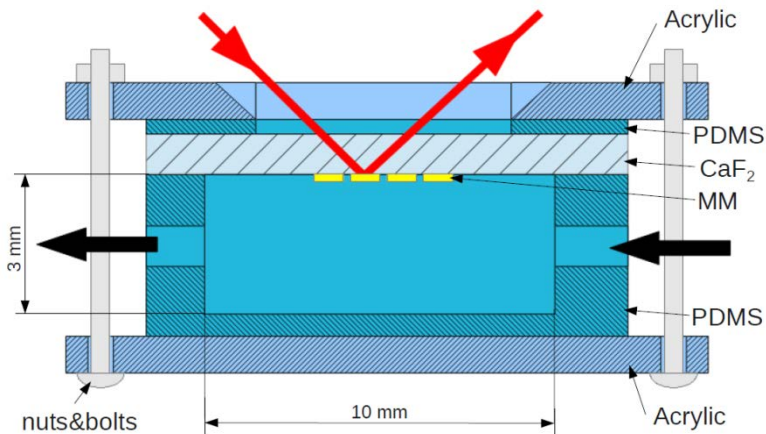
Spectral signatures of cancer cells

Outlook

The concept of a FRAMM enables plasmonic substrates that combine strong near-field enhancement, sharp spectral features and easy identification of the resonance frequency through polarized reflection spectroscopy. Designed to operate in the mid-infrared part of the electromagnetic spectrum, such substrates can be used for implementing structure-resolving label-free biosensing. Tremendous improvements in sensitivity, speed and time-resolution of biosensing can be achieved by parallel acquisition of the FTIR spectra from large functionalized arrays of narrow-band FRAMM pixels

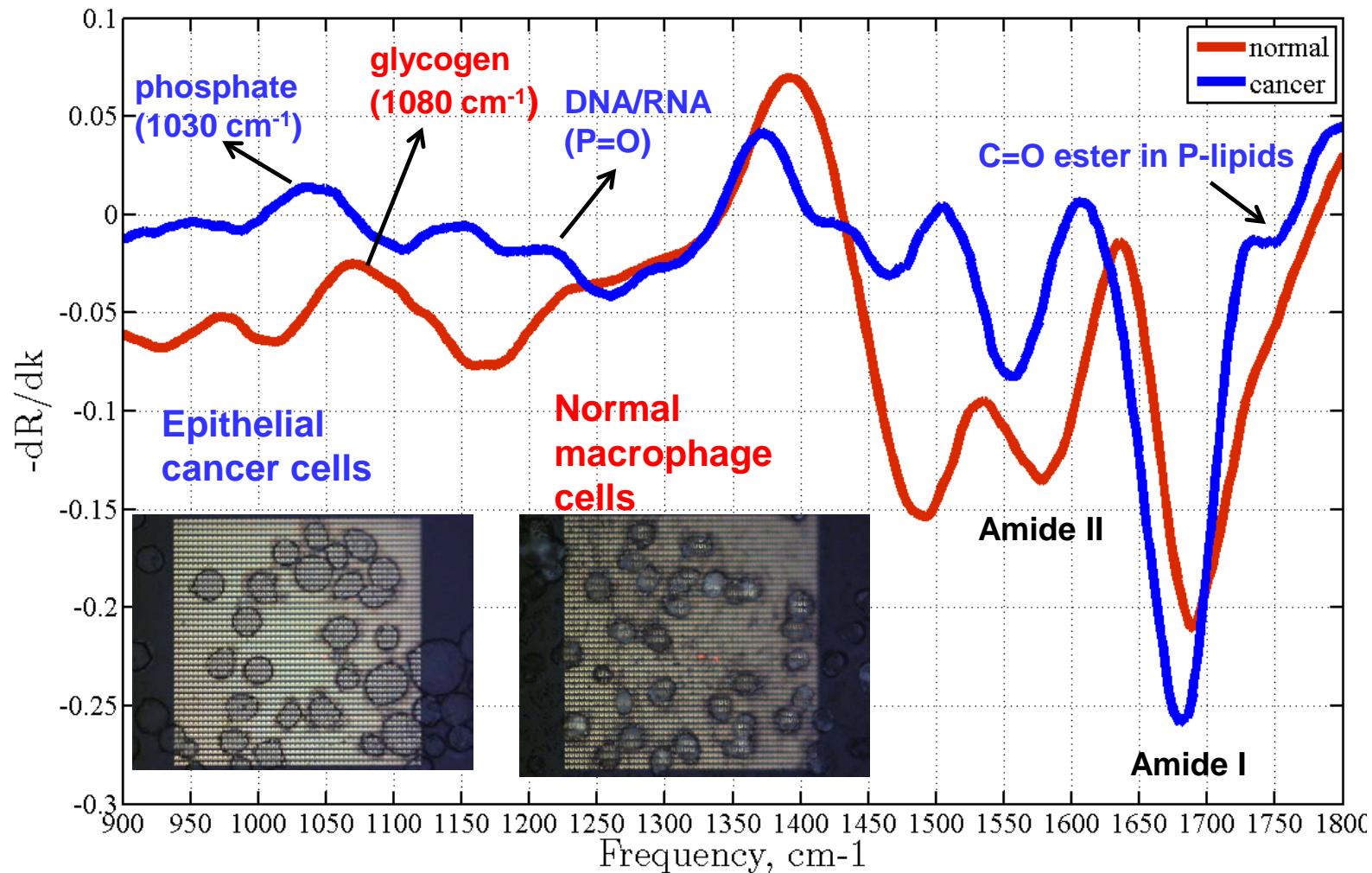
covering a significant portion of the fingerprint spectral region. By using infrared-transparent substrates, we can envision unlocking the mysteries of the conformational dynamics of biomolecules in their natural aqueous environment responsible for life-sustaining molecular binding processes.

C. Wu et.al., Nature Materials **11**, 69 (2012)





Metamaterials-Based Fingerprinting of Live Cells: Macrophages vs Malignant



Future: detection and identification of circulating tumor cells (CTCs): the key cause of cancer-related mortality because of metastasis